European Journal of Pharmaceutics and Biopharmaceutics 212 (2025) 114744

Contents lists available at ScienceDirect

European Journal of Pharmaceutics and Biopharmaceutics

journal homepage: www.elsevier.com/locate/ejpb

Small milk-derived extracellular vesicles: Suitable vehicles for oral drug delivery?

Nidhi Seegobin [a], Marissa Taub [a], Cécile Vignal [b], Christophe Waxin [b], Victoria Chris [a,c], Atheer Awad [a,d], Sudaxshina Murdan [a], Abdul W Basit [a,*]

[a] Department of Pharmaceutics, UCL School of Pharmacy, University College London, 29-39 Brunswick Square, London WC1N 1AX, United Kingdom
[b] Univ. Lille, Inserm, CHU Lille, UMR1286 - INFINITE - Institute for Translational Research in Inflammation, F-59000 Lille, France
[c] Medical Sciences Division, University of Oxford, Oxford OX3 9DU, United Kingdom
[d] Department of Clinical, Pharmaceutical and Biological Sciences, University of Hertfordshire, College Lane, Hatfield AL10 9AB, United Kingdom

ARTICLE INFO

Keywords:
Bovine milk extracellular vesicles
Hydrophilic cargo
Lipophilic cargo, Gastro-intestinal tract
Colonic Drug Delivery
Exosomes
Liposomes

ABSTRACT

Current treatments for inflammatory bowel disease often fail due to systemic side effects, but bovine milk-derived extracellular vesicles (EVs) show promise for targeted delivery to inflamed gut tissue via the leaky gut effect. This study assessed the stability of EVs as drug carriers in simulated gastrointestinal (GI) fluids and their efficacy in a colitis mouse model. EVs were characterised after incubation in PBS at various pH levels, and their lipid bilayer stability in biorelevant GI fluids was evaluated using the polar probe laurdan. Two small molecules, acridine orange (lipophilic) and riboflavin (hydrophilic), were loaded into EVs to test their release under GI conditions, while unloaded EVs were investigated for therapeutic effect via oral gavage or rectal enema in a colitis mouse model. Although no significant changes in EVs' physical properties were observed at different pH levels, lipid bilayer damage was evident in acidic ($p \leq 0.05$) and enzyme-rich environments ($p \leq 0.01$). Acridine orange release was significant ($p \leq 0.05$), but riboflavin remained encapsulated, and no therapeutic effect was observed with unloaded EVs *in vivo*. These results suggest that physical characterisation alone does not reflect EV stability, that bovine milk EVs have limited potential for oral drug delivery and are better suited for hydrophilic drugs.

1. Introduction

Inflammatory bowel disease (IBD), comprising ulcerative colitis (UC) and Crohn's disease (CD), affects over 7 million people worldwide [1,2]. Despite advances in treatment, up to 50 % of CD patients may require surgery within 10 years of diagnosis due to poor adherence caused by systemic side effects and immunogenic responses [1,2]. While most IBD therapeutics are administered orally, their systemic absorption means that only a small fraction reaches the sites of inflammation, resulting in unwanted systemic side effects [3]. Effective oral targeted drug delivery requires both the drug and its carrier to withstand the varying pH and enzymatic conditions of the gastrointestinal tract [4]. These pH changes, along with diverse enzymatic compositions, challenge the structural integrity of drugs and carriers [4,5]. Colon-targeted delivery systems are essential for increasing drug concentrations in inflamed areas, reducing systemic side effects, and improving patient adherence[6]. These systems exploit the specific physiological conditions of the colon, such as pH, microflora, and transit time [7]. Phloral® coating technology, for example, combines pH and enzymatic triggers for reliable colonic targeting [8]. However, current technologies often deliver drugs to both healthy and inflamed tissues indiscriminately. Novel approaches, such as synthetic nanoparticles (NPs), target inflamed colonic tissues by exploiting gaps in the tight junctions of the leaky gut associated with IBD [9–12]. Moreover, in IBD, goblet cell dysfunction leads to reduced mucin production and a defective colonic mucosal barrier [13–16]; allowing weakly negatively charged NPs to penetrate and bind to the positively charged proteins, such as eosinophil cationic proteins and transferrin, which are present in higher concentrations in inflamed regions [17–21]. Although synthetic NPs offer promise, clinical trials have faced challenges related to complex molecular targeting, such as the masking of targeting ligands by the formation of a protein corona or the decreased extravasation due to the impact on ligands on particle size; these issues may be mitigated by using naturally targeting nano systems such as small extracellular vesicles (EVs) derived from plants or

* Corresponding author.
E-mail address: a.basit@ucl.ac.uk (A.W. Basit).

https://doi.org/10.1016/j.ejpb.2025.114744
Received 27 February 2025; Received in revised form 8 May 2025; Accepted 9 May 2025
Available online 10 May 2025

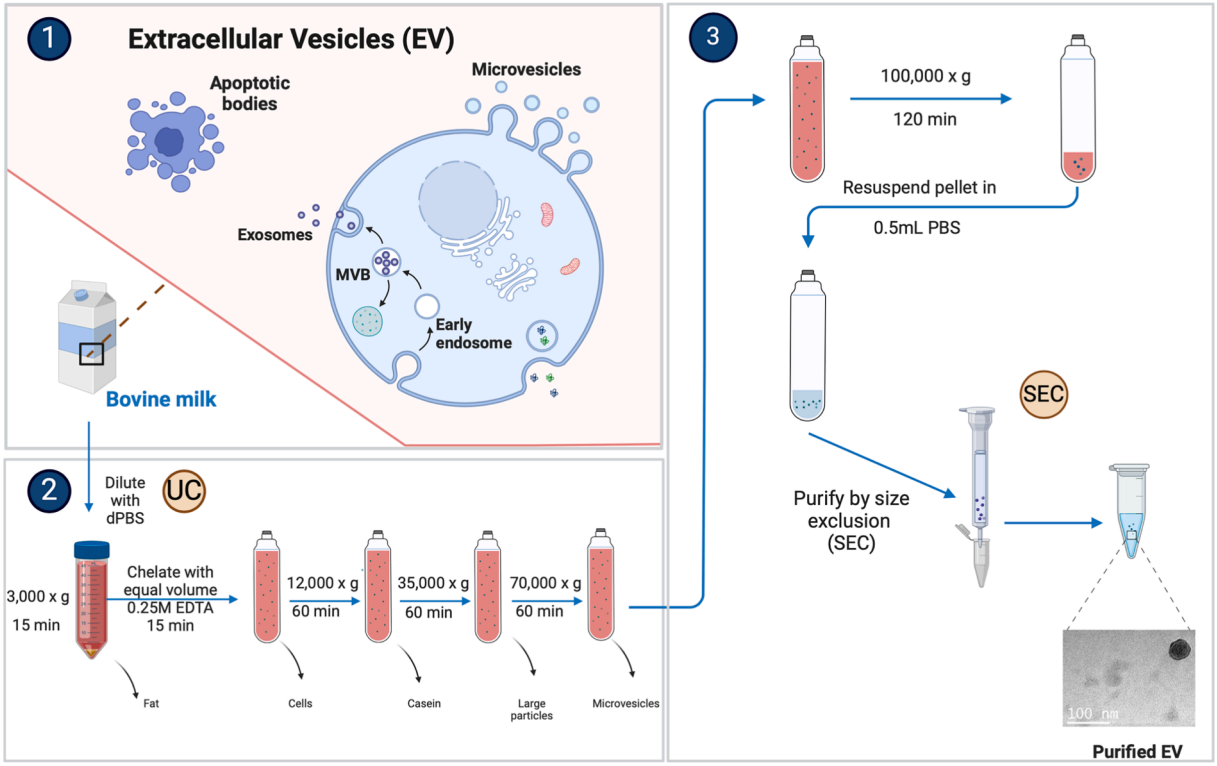

Fig. 1. Schematic diagram depicting the genesis from endosomes and multivesicular bodies (MVB) and the isolation process of EVs from milk using chelation and centrifugation then ultracentrifugation and SEC.

mammalian cells [22].

Small EVs are naturally occurring nanocarriers with high permeation and targeting abilities, making them promising candidates for targeting IBD in the GI tract [23,24]. Characterised by their small size (< 200 nm), lipid bilayer structure, and rich cargo (including nucleic acids, proteins, lipids, tetraspanins and metabolites), they offer significant potential for therapeutic delivery [25,26]. These vesicles are produced by every cell type in the body and facilitate cellular communication by transferring cargo to recipient cells via surface receptor binding or plasma membrane fusion [27,28]. Due to their natural origin, EVs are less immunogenic, well-tolerated, and can be found in various body fluids, including blood, urine, amniotic fluid, and breast milk [29]. Their transmembrane tetraspanins aid in receptor interactions, providing high biocompatibility and preferential uptake by human cells compared to synthetic NPs [30,31], making them attractive therapeutic vectors. Research has demonstrated that cow milk-derived EVs can cross the human gut epithelium intact, presenting a potential for oral therapeutic delivery [32–36]. Milk-derived EVs are a scalable EV source and exhibit cross-species tolerance without eliciting immune responses in mice [37]. Their therapeutic efficacy in treating IBD has been demonstrated in colitis mouse models [38–40], highlighting their potential as dual-function carriers to deliver innate anti-inflammatory compounds. However, the GI tract poses significant acidic and enzymatic challenges that can affect drug carriers stability, as seen with liposomes which are prone to degradation by gastric acid, digestive enzymes, and bile salts [41], leading to loss of integrity and payload breakage [42]. Due to their structural similarity to liposomes, milk-derived EV stability in the GI tract requires investigation. The stability of milk-derived EVs in oral delivery has been investigated both *in vitro*, showing resistance of milk-derived EV miRNAs and mRNAs to digestion in acidic conditions [43–47], and *in vivo*, with studies demonstrating absorption of fluorescently labelled EVs in host organs and their accumulation in the colon, highlighting their potential as oral carriers for targeting local inflammation in IBD [11,37,48–51]. Interestingly, Xu et al. (2022) found that while sublingual administration of liraglutide-loaded milk EVs effectively reduced blood glucose levels in diabetic mice, oral gavage was ineffective, suggesting differences in EV stability between salivary and gastric fluids [52]. These findings highlight discrepancies in the literature, with some studies supporting the stability of milk EVs for oral drug delivery, while others indicate accumulation in the colon or ineffectiveness via the oral route. Therefore, further research into the GI stability of EVs is critical to fully harness their potential as effective oral delivery vehicles for targeted therapies.

In the work described in this paper, our aim was to clarify EV stability in the colon and at the pH range encountered in the GI tract *in vitro* and evaluate EV efficacy *in vivo* in a mouse model. EVs were isolated from bovine milk and characterised for stability following incubation in PBS at the different pH levels found in the GI. EVs were also loaded with laurdan to assess the effect of pH and biorelevant enzymes on the lipid bilayer integrity. Hydrophilic and lipophilic drugs were loaded into milk EVs and drug release in simulated GI fluids was assessed. The therapeutic effects of orally or rectally administered milk EVs in a colitis mouse model was assessed.

2. Materials and Methods

2.1. Materials

EDTA (0.5 μM), calnexin monoclonal antibody (AF18), bovine serum albumin monoclonal antibody (3G3A2), TSG101 monoclonal antibody (4A10), CD81 monoclonal antibody (M38), magnesium sulphate heptahydrate, pepsin (MP Biomedicals), calcium chloride hexahydrate, peptone and SYBR Green PCR master mix were purchased from Thermo Fischer Scientific (Loughborough, UK). Fetal bovine serum, penicillin–streptomycin, minimum essential medium eagle, Dulbecco's phosphate buffered saline (dPBS), hemin (bovine), pancreatin from porcine pancreas 4x USP specifications, α-amylase from porcine pancreas, liposome kit: Lipid mixtures for the preparation of liposomes

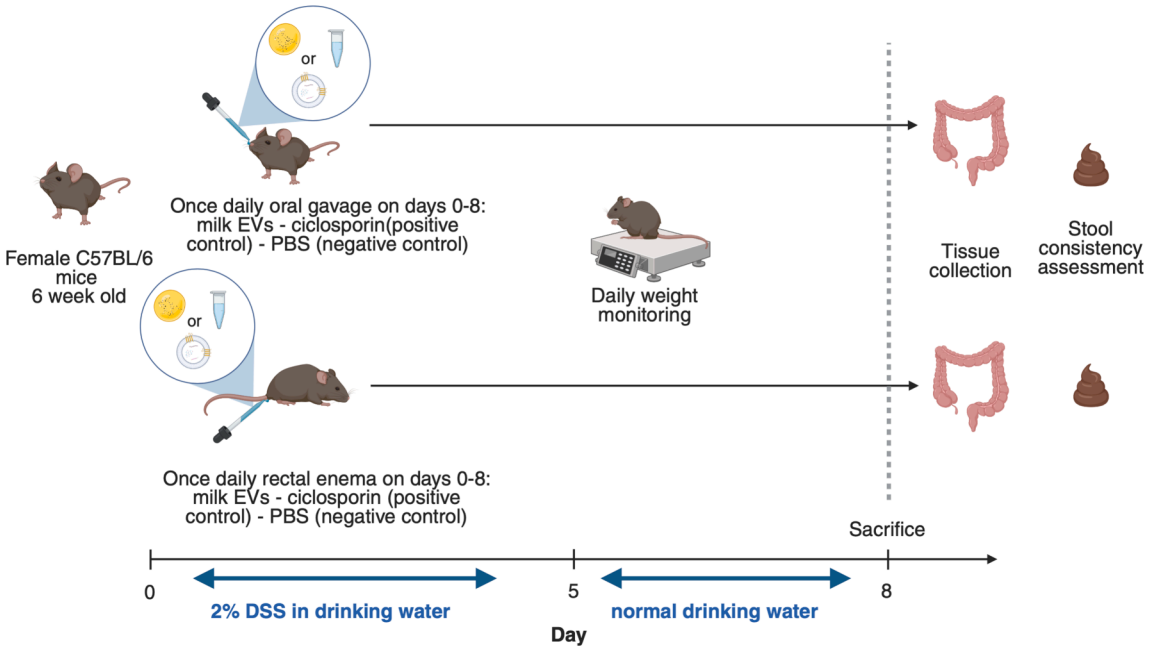

Fig. 2. Schematic representation of the *in vivo* experimental set-up for the therapeutic assay of bovine milk EVs by oral gavage or rectal enema in DSS-induced colitis C57BL/6 mice (n = 7) with a positive control (ciclosporin in an olive oil/ethanol mixture) and a negative control (dPBS).

(catalog number L4395), Millipore Sigma Amicon® Ultra centrifugal filter units (10 kDa MWCO), Tween® 20, Tween® 80, yeast extract, bile salts, L-cysteine hydrochloride, riboflavin, acridine orange, phytomenadione, hexadecyltrimethylammonium bromide, dianisidine dihydrochloride, human neutrophil MPO and vitamin K were purchased from Merck Life Science (Gillingham, UK). Other chemicals for the preparation of the simulated GI fluids include xanthan gum, potassium dihydrogen phosphate and sodium bicarbonate from VWR (Lutterworth, UK), and resazurin tablets from Scientific Laboratory supply (Fairham, UK). Fresh organic unhomogenised semi-skimmed bovine milk was obtained from a local supermarket (Dutchy organic Waitrose, UK). Size exclusion chromatography (SEC) columns qEVoriginal 35 nm Gen 2 were purchased from IZON Science Ltd. (Lyon, France). EVspin columns mini were purchased from Cambridge Bioscience (UK). Formvar/carbon on 400 mesh copper for TEM imaging were purchased from Agar Scientific LTD (UK).12—230 kDa Wes Separation Module, 8 x 25 capillary cartridges, Anti-Mouse Detection Module for Wes, Peggy Sue, and Sally Sue, were purchased from Bio Techne LTD, UK. Nucleospin RNA II kit was purchased from Macherey-Nagel (Hoerdt, France). HPLC-grade water was obtained via an ELGA HPLC water purification system (ELGA LabWater, High Wycombe, UK).

2.2. The EV isolation process

Bovine milk-derived EVs were isolated from pasteurized unhomogenized organic semi-skimmed milk, purchased from a local supermarket (Waitrose, UK), following the method by Vaswani et al. [53] (Fig. 1). 18 mL of milk was diluted with 30 mL of PBS and centrifuged at 3,000 × g for 15 min to pellet cells and cellular debris. The supernatant was mixed with an equal volume of 0.25 M EDTA and incubated on ice for 15 min to chelate casein-calcium complexes. The mixture then underwent successive ultracentrifugation steps at 12,000 × g, 35,000 × g, and 70,000 × g, each for 1 h (Sorvall WX80 + Thermo Fisher Scientific and Optima L-90 K, Beckman Coulter), to remove protein aggregates and larger vesicles. After each step, the supernatant was filtered through 0.22 μm syringe filters. Finally, the supernatant was ultracentrifuged at 100,000 × g for 2 h to pellet the milk EVs. The EV pellets were resuspended in 500 μL of PBS and further purified using a qEV Gen2 SEC column (35 nm pore size, Izon, Lyon, France), collecting 2000 μL fractions. The final EV fractions were concentrated to 500 μL and stored at − 80 °C for downstream applications.

2.3. Preparation of simulated gastro-intestinal (GI) fluids

2.3.1. dPBS at physiologically relevant pHs

Dulbecco's Phosphate Buffered Saline (dPBS) was adjusted to different pH values (1.2, 6.8, 7.0, 7.4) using 1 M hydrochloric acid (HCl) and 1 M sodium hydroxide (NaOH).

2.3.2. Simulated stimulated saliva fluids (SSSF)

SSSF was selected for this study as it simulates saliva produced in response to stimuli such as taste, chewing, or other sensory inputs, making it most suitable for assessing the stability of a medicinal carrier compared to unstimulated saliva and was prepared according to a protocol by Ali et al.: Xanthan gum (0.05 g) was dissolved in 6.892 mL of pH 7.4 buffer, followed by the addition of 1 g porcine gastric mucin, 100 mg porcine amylase, and 5.6 μL of Tween 20. The volume was made up to 100 mL with deionised water, and the pH was adjusted to 7.4 [54].

2.3.3. Simulated gastric fluids (SGF) for the pH and laurdan stability assays

For the pH and laurdan stability assays, SGF was prepared according to a USP specifications protocol by Wang et al. [55]. Sodium chloride (0.2 g) was dissolved in 50 mL of water, and 0.7 mL of 10 M HCl was added to adjust the pH to 1.2. Pepsin (0.32 g) was then added, and the volume was made up to 100 mL with water. Pepsin was added only after the pH adjustment to avoid enzyme degradation. For the acridine orange and riboflavin release assays, fasted state simulated gastric fluid (FaSSGF) was prepared according to a previously described protocol [56] by dissolving 80 μM sodium taurocholate and 20 μM lecithin in deionised water. This was followed by the addition of 0.1 mg/mL pepsin, 34.2 mM sodium chloride, and 100 μg/mL lipase from porcine pancreas. The pH was adjusted to 1.20 using HCl and thoroughly mixed.

2.3.4. Simulated intestinal fluids (SIF) for the pH and laurdan stability assays

For the pH and laurdan stability assays, SIF was prepared according to a USP specifications protocol by Wang et al. [55]. Monobasic

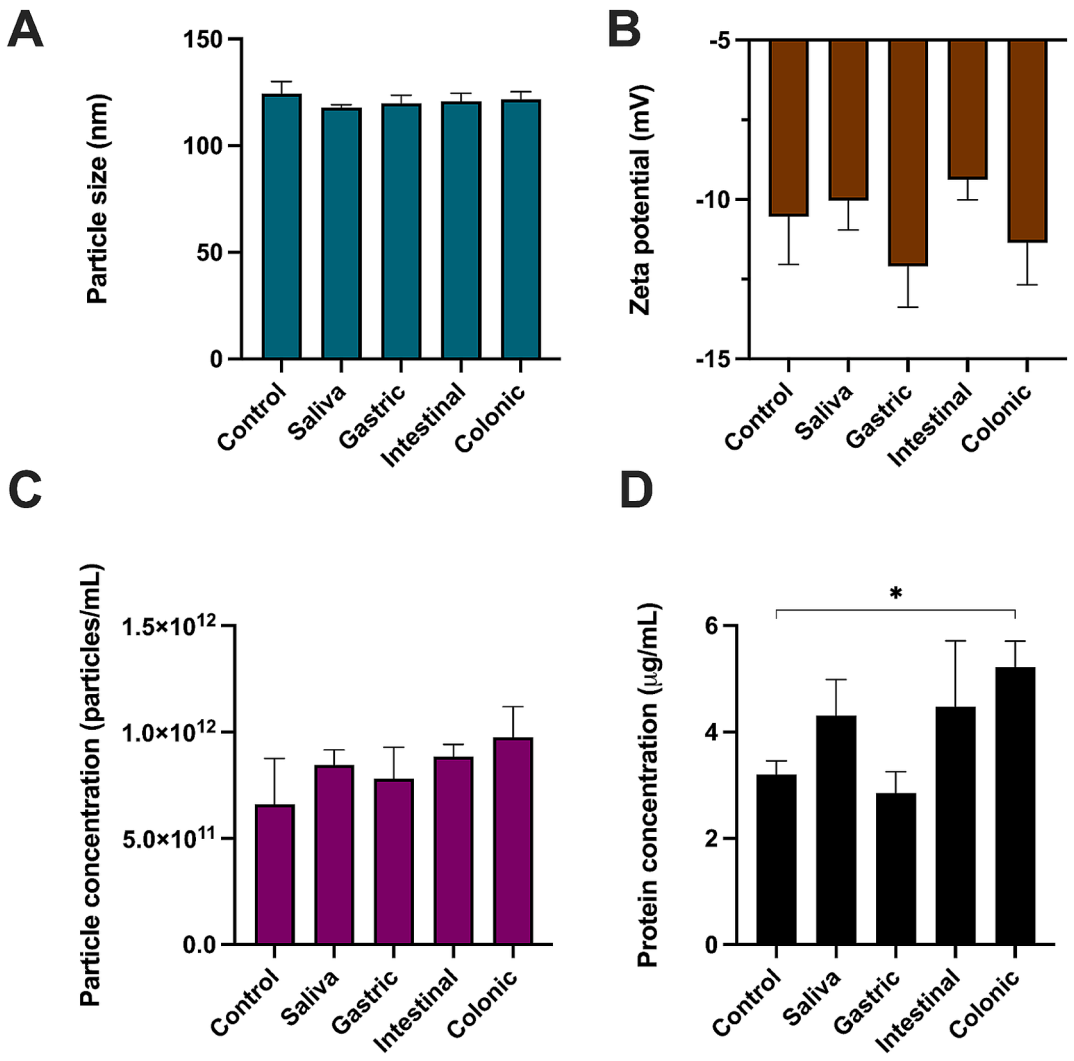

Fig. 3. (A) Particle size (NTA peak mean), (B) ζ potential, (C) particle concentration and (D) protein concentration of milk EVs following exposure to PBS at physiologically relevant GI pH (n = 3).

potassium phosphate (0.68 g) was dissolved in 25 mL of water, then 7.7 mL of 0.2 N NaOH was added to adjust the pH to 6.8. Pancreatin (1 g) was added, gently shaken until dissolved, and the volume adjusted to 100 mL with water. Pancreatin was added after pH adjustment to prevent enzyme precipitation.

For the acridine orange and riboflavin release assays, fasted state simulated intestinal fluid (FaSSIF) was prepared according to a previously described protocol [56] by dissolving 3 mM sodium taurocholate and 0.75 mM lecithin in deionised water. This was followed by the addition of 28.65 mM potassium dihydrogen phosphate, 105.85 mM sodium chloride, and 20 mg/mL lipase from porcine pancreas. The pH was adjusted to 6.80 using HCl or NaOH as necessary.

2.3.5. Simulated colonic fluids

Peptone and yeast extract (2 g each) were weighed into a glass flask containing distilled water (500 mL). Calcium chloride hexahydrate (0.01 g), potassium dihydrogen phosphate (0.04 g), magnesium sulphate heptahydrate (0.006 g), and sodium chloride (0.1 g) were added into the flask and dissolved by stirring. Tween 80 (2 mL), l-cysteine HCl and bile salts (0.5 g each) were then added and subsequently dissolved in the same solution. Into this, hemin (0.005 g in two drops of 1 M NaOH), 0.025 % (w/w) resazurin in deionized water solution (4 mL), and vitamin K (10 μL) were added under stirring. Upon dissolution, sodium bicarbonate (2 g) and distilled water were added to make the final volume of solution up to 1000 mL. The pH of this solution was subsequently adjusted to 6.8 using 0.1 M HCl or 1 M NaOH solutions.

2.4. Characterisation of EVs

2.4.1. Protein quantification

The protein concentration of EVs was quantified by the bicinchoninic acid (BCA) assay using the Pierce™ BCA Protein Assay Kit (Thermo Fisher, UK) according to the manufacturer's protocol. Purified EV samples for BCA were prepared by a 1:3 dilution in dPBS. BCA working reagent was prepared by mixing reagents A and B in a 50:1 ratio. A standard curve was generated using bovine serum albumin (BSA) standards, and absorbance was measured at 600 nm after a 2-hour incubation at 37 °C.

2.4.2. Zeta potential of EVs

The zeta (ζ) potential of the EVs was measured using Dynamic Light Scattering (DLS) with a Malvern ZetaSizer (Malvern Panalytical Ltd., Malvern, UK). EV samples (100 μL) were diluted in deionised water (900 μL) and measurements (n = 3) were conducted at 25 °C with an equilibration time of 120 s. The measurement settings were 173° backscatter (NIBS default), with an automatic measurement duration.

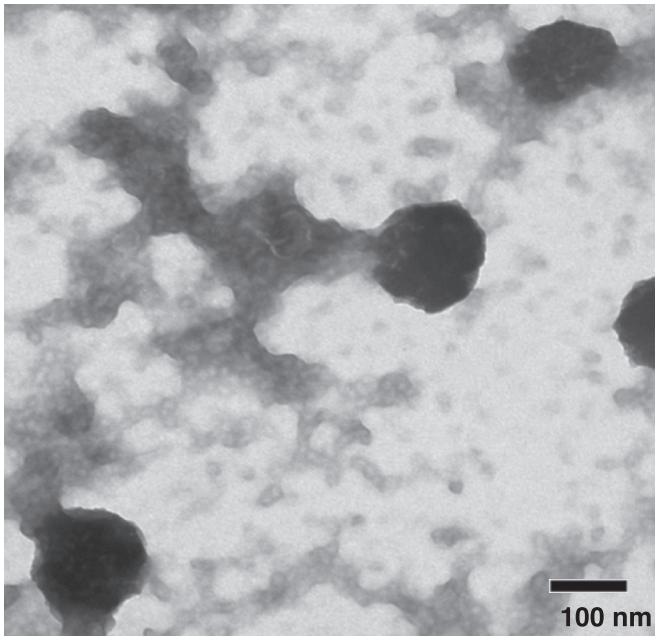

Fig. 4. Example of TEM images of bovine milk EVs obtained for the physical characterisation study following incubation in dPBS at pH 1.2.

Table 1
Characterisation of bovine milk-derived EVs isolated for the laurdan, release and animal studies.

Study	Size (nm)	ζ potential (mV)	Particle concentration (particle/mL)	Protein concentration (μg/mL)	Particle to protein ratio (particle/μg)
Laurdan study	159 ± 6	−14 ± 0	6E + 12 ± 3E + 11	1260 ± 9	5E + 09 ± 2E + 08
Release study	111 ± 4	−14 ± 1	7E + 12 ± 7E + 11	1610.6 ± 30	4E + 09 ± 8E + 07
Animal study	116 ± 1	−12 ± 0	7E + 12 ± 3E + 11	1632 ± 266	5E + 09 ± 2E + 08

2.4.3. Nanoparticle-Tracking analysis (NTA)

NTA was conducted using a Nanosight LM14C, equipped with a green laser (532 nm) and NanoSight NTA 3.4 software (Malvern Panalytical, Ltd., UK). EV samples were diluted in PBS to achieve an optimal concentration for detection (typically around 10^8 particles/mL). Each sample was measured five times, with videos recorded for 90 s each, yielding a size distribution based on hydrodynamic diameter and particle concentration.

2.4.4. Transmission electron microscopy (TEM) imaging

Concentrated EV samples were prepared for electron microscopy by fixing them onto Formvar-carbon coated EM grids (Agar Scientific, Stevenage, UK). The grids were placed on a 10 μL droplet of EV sample for 30 s. Following this, the grids were transferred to a 4 % (w/v) aqueous uranyl acetate droplet for 90 s to stain the samples. The grids were then subjected to two washes by placing them on deionised water droplets for 30 s each. After washing, the grids were carefully dried by blotting with filter paper and allowed to air dry completely at room temperature. Imaging was conducted using a JEOL 1400 Plus electron microscope operated at an accelerating voltage of 120 kV. The microscope was equipped with a Gatan Rio16 camera and used the Digital Micrograph® software (Version 3.5, Gatan Microscopy Suite, California, USA) for image acquisition and analysis. Magnification settings ranged from 35,000x to 60,000x to capture detailed images of the EVs.

2.4.5. Characterisation of EV protein markers

Western blotting was performed using the Wes ProteinSimple (Bio-Techne, Minnesota, USA) following the manufacturer's instructions, utilizing a 12–230 kDa Separation Module and the anti-mouse detection module. EV samples were first concentrated to 3 μg/μL and then lysed by mixing with equal volumes of RIPA buffer, followed by incubation on ice for 20 min. The lysed EV solution, at a concentration of 1.5 μg/μL, was added to a Fluorescent Master Mix at a 4:1 ratio and heated at 95 °C for 5 min. Subsequently, the prepared samples, along with blocking reagent, primary antibodies (diluted in antibody diluent buffer), HRP-conjugated secondary antibodies, and chemiluminescent substrate, were loaded into the plate provided in the Separation Module. The instrument was operated using the default settings: stacking and separation at 475 V for 30 min; blocking reagent for 5 min, primary and secondary antibody both for 30 min; Luminol/peroxide chemiluminescence detection for approximately 15 min (exposures of 1–2-4–8-16–32-64–128-512 s). The resulting electropherograms are then used for automatic peak detection.

2.5. Laurdan dye analysis of EVs and liposomes to assess bilayer integrity

Liposomes were used as a positive control in this study. The liposome suspension was produced according to the instructions of the liposome kit: Lipid mixtures for the preparation of liposomes (Sigma-Aldrich, catalog number L4395). The lipids were hydrated in 1 mL of deionised water, resulting in the following composition: L-α-phosphatidylcholine (63 μmol/mL), stearylamine (18 μmol/mL), and cholesterol (9 μmol/mL). The suspension was then passed through polycarbonate membranes with pore sizes of 200 nm and 100 nm sequentially using an extruder (Avanti Polar Lipids). Each sample was extruded a total of 20 times through each membrane at 37 °C to produce unilamellar vesicles around 100 nm in size. Laurdan dye (0.1 μmol/L) was added to milk EVs (1200 μg) and liposomes (600 μL) suspended in 0.5 mL buffer solution at the relevant pH and in simulated gastrointestinal fluids, as schematically shown in **Supplementary Fig. S2**. The mixtures were incubated at 37 °C for 1 h in the dark. The buffer solutions used included PBS at various pH values and simulated gastrointestinal fluids prepared according to standard protocols to mimic the conditions of the gastrointestinal tract. After incubation, the laurdan excitation spectra were recorded using a SpectraMax (M2e, Molecular Devices, USA) set at an excitation wavelength of 340 nm, with emission spectra collected at 435 nm and 490 nm at 37 °C. The generalised polarisation (GP) values were calculated according to the equation: $GP = (I_{435}–I_{490})/(I_{435} + I_{490})$, where I_{435} and I_{490} are the emission intensity of 435 and 490 nm, respectively. Each measurement was performed in triplicate to ensure reproducibility. Controls included buffer solutions without EVs or liposomes to account for background fluorescence.

2.6. Assessment of the encapsulation stability of hydrophilic and lipophilic cargo stability in milk EVs

2.6.1. Loading of riboflavin and acridine orange into milk EVs

The hydrophilic drug riboflavin (logP −1.5111; 1.2 mg/mL) was dissolved in deionised water to create a supersaturated solution. This solution was then filtered using a 0.22 μm filter and added to milk EVs (3750 μg/mL). The EVs-drug mixture was sonicated using a Soniprep 150 with the following settings: 20 % amplitude, 6 cycles of 30 s on/off for three minutes, with a 90-second cooling period between each cycle. Following sonication, the milk EVs loaded with riboflavin (milk EVs_R) were incubated at 37 °C for 2 h to allow the EV membranes to recover and then isolated from unentrapped riboflavin through a qEV Gen2 SEC column (35 nm pore size, Izon, Lyon, France). For the lipophilic drug acridine orange (AO), milk EVs (3750 μg/mL) were loaded by passive diffusion, following the method of Agrawal, A. K. et al. [37]. The milk EVs were incubated with a 100 μg/mL solution of AO (logP 3.4112) in ethanol for 30 min at room temperature, the final solvent concentration was maintained at 10 % (v/v). After 30 min, the milk EVs loaded with

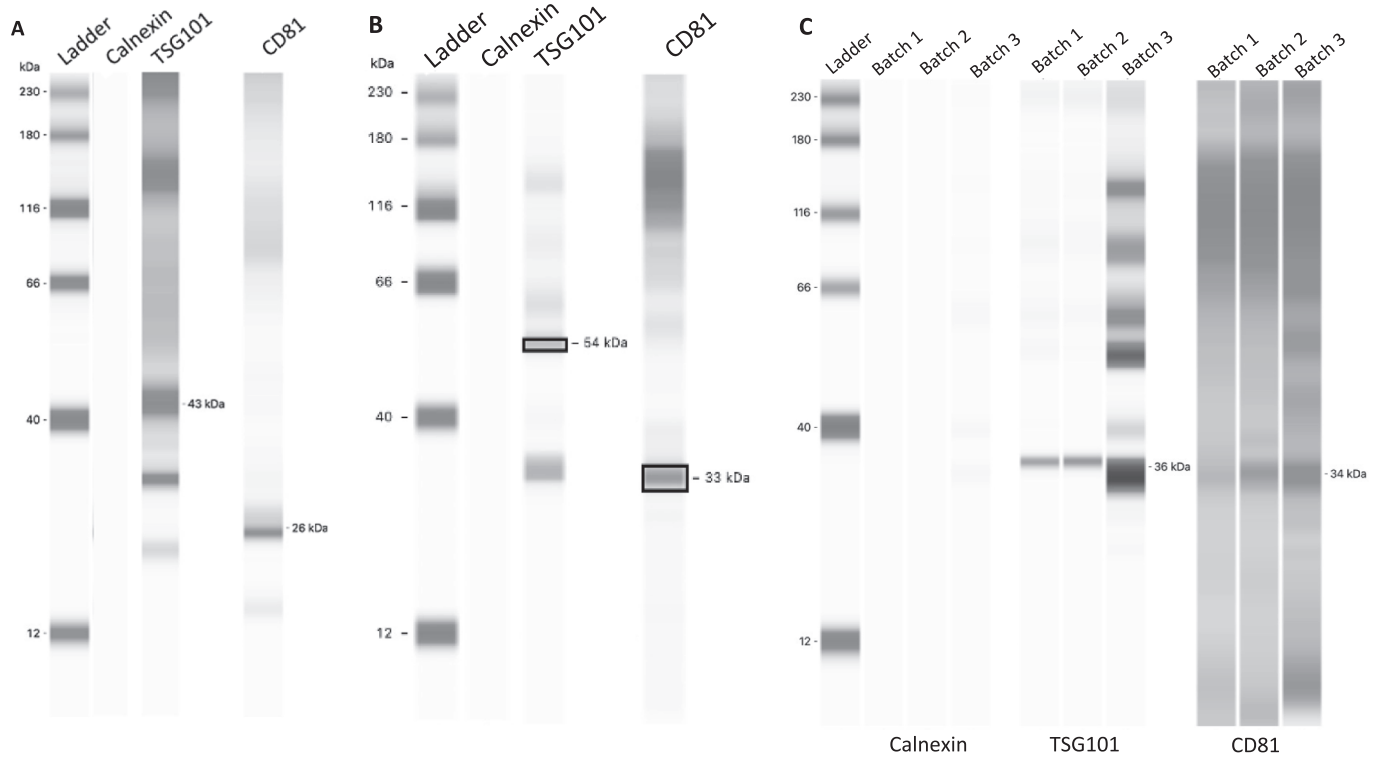

Fig. 5. Western blot results for bovine milk derived EVs used in (A) the laurdan assay, with no detected bands for calnexin and showing bands TSG101 at 43 kDa and CD81 at 26–30 kDa; (B) the release study, with no bands for calnexin and bands for TSG101 at 54 kDa and CD81 at 33 kDa; (C) the *in vivo* study, with three different batches showing no bands for the negative control calnexin and bands for TSG101 at 36 kDa and bands for CD81 at 34 kDa (n = 3).

AO (milk EVs_{AO}) were isolated from unentrapped AO through a qEV Gen2 SEC column (35 nm pore size, Izon, Lyon, France). The loading efficiency of Acridine Orange and Riboflavin were found to be 0.025 % and 0.008 %, respectively.

2.6.2. Determination of drug location with a Bligh & Dyer assay

Lipid and aqueous phase extraction for localisation of acridine orange and riboflavin was performed using the Bligh and Dyer method with the use of methanol and chloroform [57]. Methanol was added to riboflavin in water (0.012 mg/mL) and AO in ethanol (0.1 μg/mL) solutions at a 2:1 vol ratio and vortexed thoroughly. Chloroform was then added at a 1:1 ratio (chloroform: methanol), followed by another vortex mixing. Water was added to the mixture at a 2:2:1.8 ratio (chloroform: methanol: water), and the mixture was vortexed again before centrifugation at 1,000 × g for 10 min to facilitate phase separation. The contents of each phase were analysed against a blank with excitation wavelengths of 490 nm for acridine orange and 450 nm for riboflavin using a fluorescent plate reader (SpectraMax M2e, Molecular Devices, USA).

2.6.3. Acridine orange and riboflavin release study

The release of acridine orange and riboflavin from milk EVs was measured as schematically shown in **Supplementary Fig. S2**. Milk EVs loaded with riboflavin (milk EVs_R) and acridine orange (milk EVsAO) were incubated in dPBS at relevant gastrointestinal (GI) pH and simulated fluids at 37 °C for 1 h. Following incubation, the samples were subjected to size exclusion using EV-spin 96 columns (Cell Guidance Systems, UK). The collected fractions were analysed using a plate reader (SpectraMax M2e, Molecular Devices, USA) with excitation wavelengths of 490 nm for acridine orange and 450 nm for riboflavin, both at 37 °C.

2.7. In vivo assessment of the therapeutic efficacy of milk EVs

2.7.1. Study design for the efficacy evaluation of milk EVs in a DSS-induced colitis mouse model

Female C57BL/6 mice aged 6 weeks (Janvier Labs, Le Genest-Saint-Isle, France) were housed under standard conventional conditions. Mice experiments were performed in accordance with the approval (Authorisation No. 7267–2016100410284439) from the Ethics Committee in Animal Experimentation Nord-Pas de Calais (CEEA75) which was approved by the French ministry for higher education and research. The CEEA75 carries out its activity according to the principles of European directive 2010/63/EU (transposed into French law 2013/2/1/AGRG1238767A) and the "National Charter on the ethics of animal experimentation" while respecting the recommendations for specific procedures issued by the National Ethics Reflection Committee on animal experimentation.

Mice (n = 7 per group) received bovine milk EVs (1 mg/mouse/day) once daily by oral gavage (100 μL) or by rectal enema (50 μL) for 8 consecutive days, as schematically shown in Fig. 2. Ciclosporin (70 mg/Kg/day) dissolved in an olive oil/ethanol mixture (9:1 v/v) was used as a positive control, and dPBS was used as a negative control also administered by oral gavage (100 μL) or by rectal enema (50 μL) once daily for 8 consecutive days. DSS in drinking water (2 % w/v) was used to induce colitis over the course of the first 5 days. Throughout the total 8 days of the study, mice were monitored daily for weight, stool consistency and for the presence of blood in their faeces. The Disease Activity Index (DAI) was used to assess disease severity based on weight loss, faecal consistency, and rectal bleeding, with scores ranging from 0 to 8, where higher scores indicate greater disease activity. Weight loss was scored as follows: 0 = <1 %, 2 = 1–5 %, 3 = 5–10 %, and 4 = >10 %. Faecal consistency was scored from 0 to 3, with 0 indicating normal pellets, 1 = moderate soft pellets, 2 = partly formed stool, and 3 = watery diarrhoea. Bleeding was scored as 0 = no visible blood, 1 = visible blood in faeces and 2 = rectal bleeding. On Day 8, mice were sacrificed, dissected, and

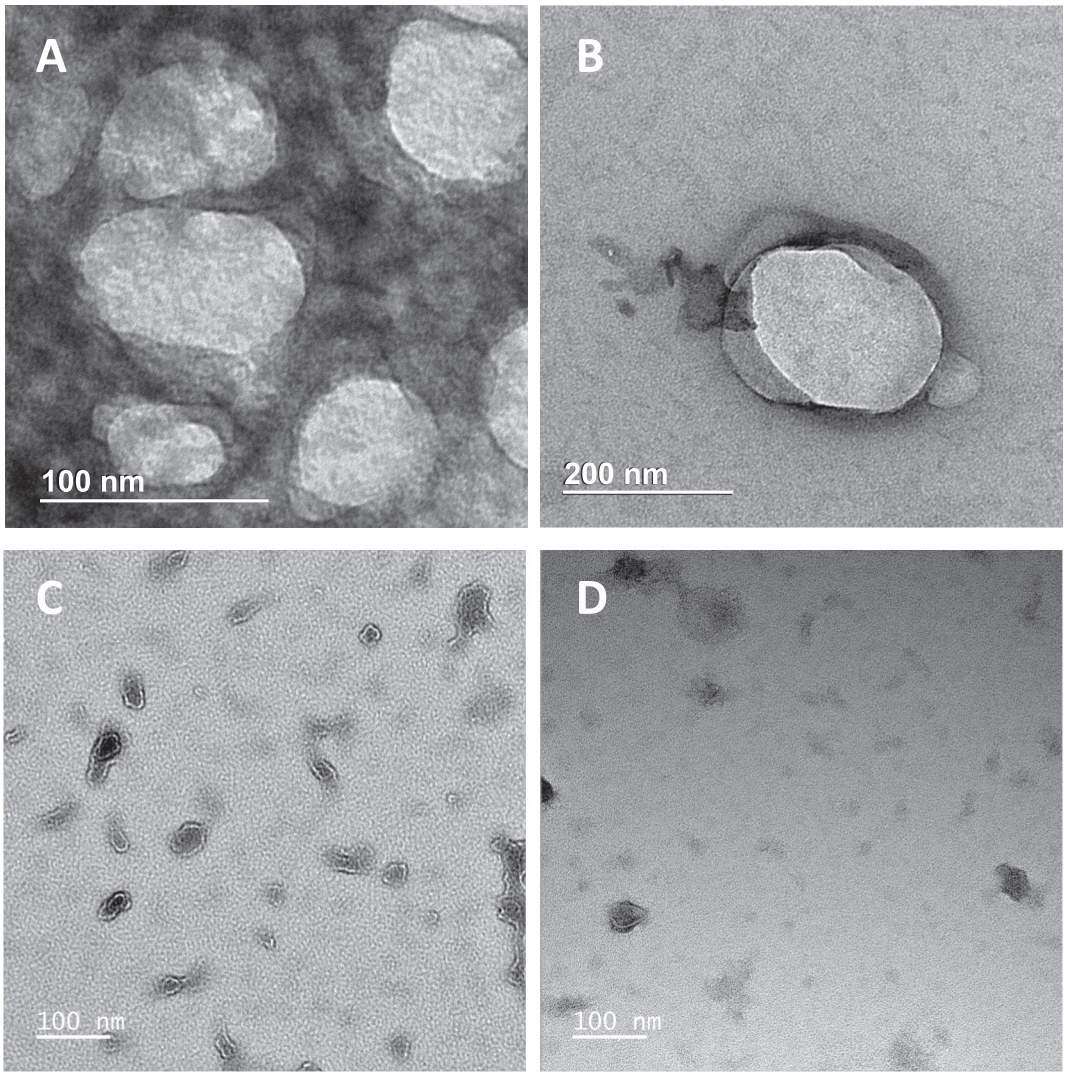

Fig. 6. TEM images of bovine milk derived EVs (A) and liposomes (B) as a negative control used in the laurdan study, milk EVs used in the drug release study (C) and milk EVs used in the *in vivo* study (D).

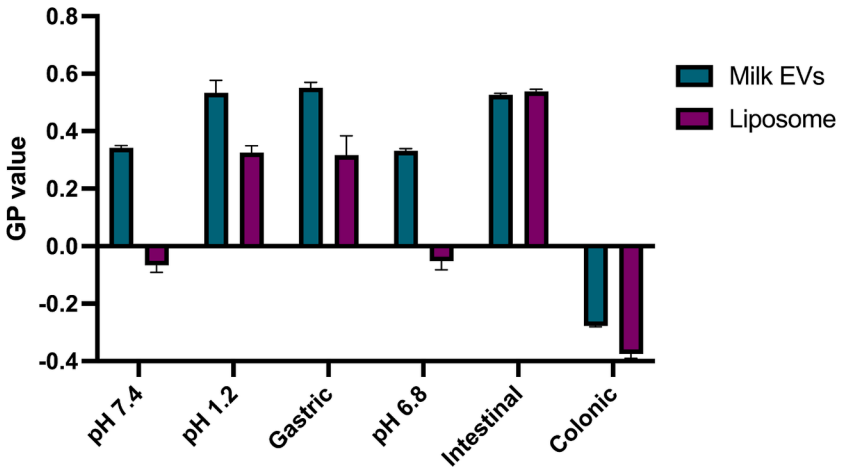

Fig. 7. Bar chart showing the laurdan GP values in different fluids for milk derived EVs and liposomes following exposure to various simulated fluids (n = 3). Statistically significant increases in GP values were observed upon exposure to PBS at pH 1.2 ($p < 0.05$), simulated gastric fluid ($p < 0.01$), and simulated intestinal fluid ($p < 0.001$) compared to the control condition (PBS, pH 7.4). No significant changes were observed in either EVs or liposomes at pH 6.8.

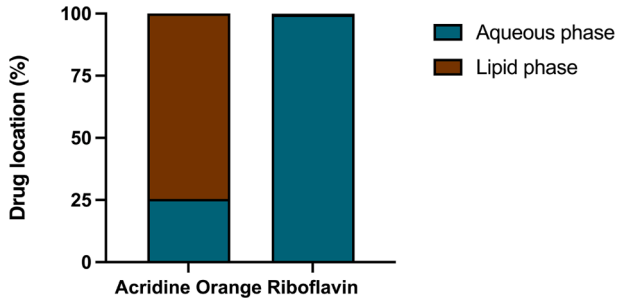

Fig. 8. Stacked bar graph depicting the location of recovered acridine orange and riboflavin following a Bligh & Dyer test (n = 2). The majority of riboflavin was recovered in the aqueous phase, while approximately 75 % of acridine orange was found in the lipid phase. (For interpretation of the references to colour in this figure legend, the reader is referred to the web version of this article.)

colonic tissues were collected from the visibly diseased areas, identified by oedema in the DSS model, and used for microscopic analyses and the detection of inflammatory markers.

2.7.2. Histology

For histological analysis, colon tissues were fixed in 4 % paraformaldehyde overnight, embedded in paraffin, and sectioned. Sections were stained with May-Grünwald Giemsa (MGG) and scored for the presence of inflammatory cells and tissue damage. Scores ranging from 0 to 6, where higher scores indicate greater colitis. Inflammation was scored on a scale of 0 to 3, with 0 = no inflammation, 1 = increased inflammatory cell infiltrate in the lamina propria, 2 = increased inflammatory cell infiltrate in the sub-mucosa, and 3 = transmural inflammatory cells. Tissue damage was assessed on a scale of 0 to 3, where 0 = no mucosal damage, 1 = increased number of intraepithelial lymphocytes (mild epithelial damage), 2 = erosions and crypt abscesses (moderate epithelial damage), and 3 = ulcerations (severe epithelial damage). All scoring was performed in a blinded manner by an experienced investigator.

2.7.3. qPCR quantification of inflammatory markers

Colonic tissue samples underwent total ribonucleic acid (RNA) extraction using a Nucleospin RNA kit in accordance with the manufacturer's guidelines (Macherey-Nagel, Düren, Germany). Subsequent reverse transcription was conducted utilising a High-Capacity cDNA Archive Kit, followed by quantitative polymerase chain reaction (qPCR) using SYBR Green (Thermo Fisher Scientific). Primer sequences were designed utilising Primer Express 3 (v3.0.1, Thermo Fisher Scientific). Melting curve analyses were performed for each sample and gene to validate the specificity of amplification. Quantification of target gene expression relied on the comparative cycle threshold (Ct) value, with fold changes in target genes determined utilising the $2^{-\Delta\Delta Ct}$ method.

2.7.3.1. Myeloperoxidase (MPO) activity for immune system activation assay. MPO is present within neutrophils and is released when the immune system is activated thereby acting as a biomarker of inflammation [58]. Mice colons were homogenised in a 0.5 % (w/v) hexadecyltrimethylammonium bromide solution in 50 mM PBS. They were then subjected to three cycles of freeze-thawing followed by centrifugation at 14,000 × *g* for 15 min at 4 °C. MPO activity was assessed in the resulting clear supernatant by adding dianisidine dihydrochloride at a concentration of 1 mg/mL along with 5×10^{-4} % (w/v) hydrogen peroxide (H_2O_2). The change in optical density was measured at 450 nm. Human neutrophil MPO served as the standard reference. MPO activity was quantified in terms of units, where one unit of MPO activity corresponded to the degradation of 1.0 μmol of peroxide per minute at 25 °C. To standardise the readings from tissue samples, MPO activity was normalised to the total protein content, which was determined using the DC™ protein assay (Bio-Rad, France).

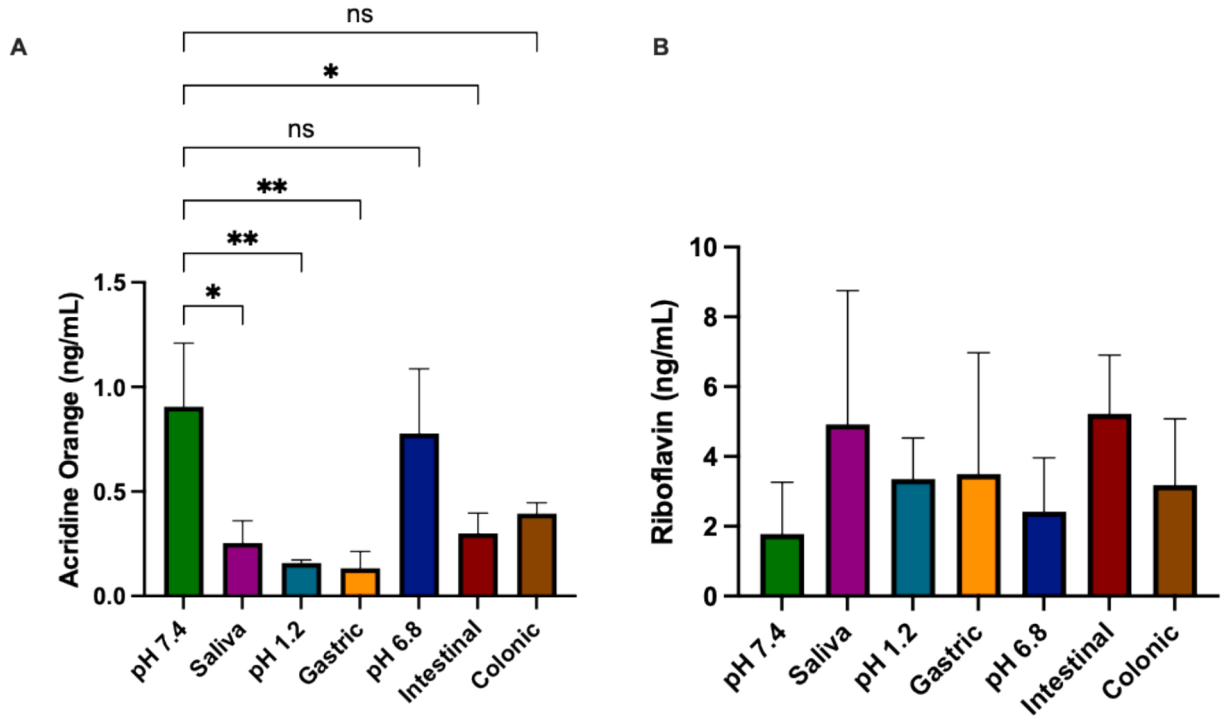

Fig. 9. Bar charts depicting the concentration of acridine orange (A) and riboflavin (B) loaded milk EVs remaining after incubation in GI fluids (n = 3). The fluorescence in PBS at pH 7.4 is the control. (For interpretation of the references to colour in this figure legend, the reader is referred to the web version of this article.)

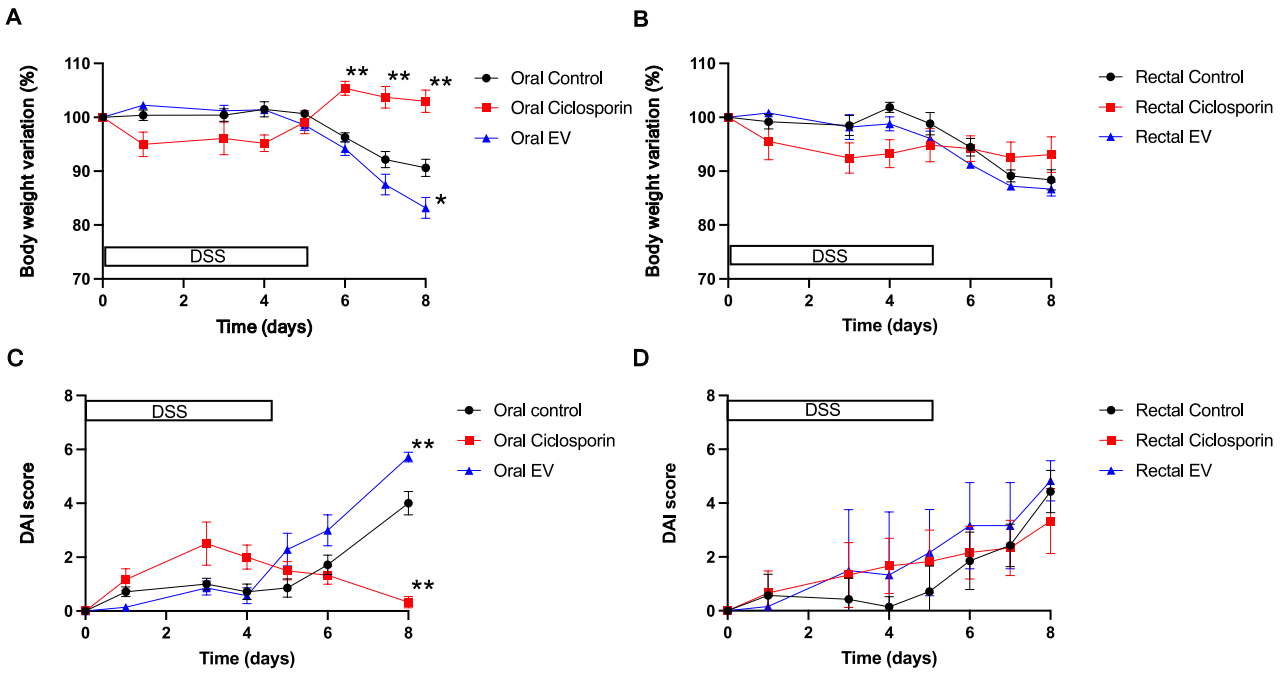

Fig. 10. Percentage change in body mass of the DSS-treated mice following administration of either PBS, ciclosporin or EVs by (A) oral gavage or (B) rectal enema and the Disease Activity Index (DAI) scores following (C) oral and (D) rectal administration (n = 7).

2.8. Statistical analysis

GraphPad Prism (Version 10.1.1, GraphPad Software LLC, California, USA) was used to plot figures and perform statistical tests. All *in-vitro* analyses were performed using one-way ANOVA followed by Tukey's post hoc test as a comparison between the control fluid (PBS at pH 7) and all relevant GI fluids. Differences between study arms for the *in vivo* assays were assessed using the Mann-Whitney *U* test to account for any animal losses and to evaluate the differences between two independent variables without assuming a normal distribution of the data. This approach provided a robust and reliable comparison across all treatment groups and time points. In all cases, $p \leq 0.05$ was considered significant. Significance markers were used accordingly on plots: * $p \leq 0.05$, ** $p \leq 0.005$ and *** $p \leq 0.001$. Unless stated otherwise, bar on charts and points on plots represent mean values and error bars represent standard deviation.

3. Results and discussion

3.1. Vesicle stability measured via physico-chemical properties

Following EV incubation in PBS at physiologically relevant GI pHs (pH 7 for the control, pH 7.4 for saliva, pH 1.2 for gastric and pH 6.8 for intestinal and colonic) [59], their size (see Fig. 3**A**), ζ potential (see Fig. 3**B**), particle concentration (see Fig. 3**C**) and protein concentrations (see Fig. 3**D**) were measured.

The stability of milk EVs was assessed across physiologically relevant GI pH levels using one-way ANOVA. There were no observed statistically significant ($p > 0.05$) differences in size, ζ potential, or particle concentration. However, a significant ($p < 0.05$) difference was found in protein concentration. A Tukey post hoc test indicated that the colonic pH group had a significantly ($p < 0.05$) higher protein concentration compared to the control group, and no significant ($p > 0.05$) differences between the control and saliva groups, control and gastric groups, and control and intestinal groups. These results indicate that pH does not affect the physical characteristics of EVs and may potentially indicate stability. The observed increase (> 2-fold) in protein concentration for milk EVs at colonic pH is surprising and likely due to an error as this was not seen at intestinal pH, despite both colonic and small intestinal conditions using only dPBS at pH 6.8. TEM images confirmed the presence of small EV-sized particles with lipid bilayers (see Fig. 4) but did not reveal differences between particles exposed to different GI pH levels.

These results are in accordance with other studies investigating the structural stability of EVs based on variations in EV size and polydispersity index (PDI) [37,44,60]. Further assessments of EVs in simulated GI fluids using physiologically relevant enzymes was impeded by residual GI proteins, specifically when using pepsin for gastric fluids and pancreatin for intestinal fluids. These residual proteins interfered with protein concentration measurements using the BCA assay following SEC. According to the Minimal information for studies of extracellular vesicles (MISEV) 2023 guidelines, comprehensive EV characterization requires total protein quantification [25]. However, the use of ExoSpin96 for EV isolation resulted in the co-elution of a significant proportion of simulated GI enzymes, as ExoSpin96 retains only approximately 95 % of proteins. This considerable extent of GI enzymes elution complicated the accurate protein concentration analysis of the EVs. Therefore, alternative approaches are required to assess EV stability whilst in the presence of these enzymes. This can be achieved by continuing with traditional EV characterisation techniques, while adding phospholipid quantification [61], or by loading the EVs with fluorescent probes or a drug payload for stability evaluation.

3.2. Physical characterisation of EVs prior to subsequent assays

Milk EVs were characterised for their size, ζ potential, particle concentration and protein concentration prior to loading with laurdan, hydrophilic and lipophilic cargo for the release assay and prior to administration in the in-vivo assay (see Table 1). The presence of specific protein markers, including CD81 and TSG101 and the absence of Calnexin was confirmed using Western blot analysis for the Laurdan assay (see Fig. 5**A**), the release study (see Fig. 5**B**) and the *in vivo* study (see Fig. 5**C**). Additionally, the structural integrity of the EVs was verified through TEM, which revealed their characteristic cupped shape and lipid bilayer structure as shown by the visible thin electron-dense boundary around the vesicle for the laurdan assay (see Fig. 6 **A&B**),

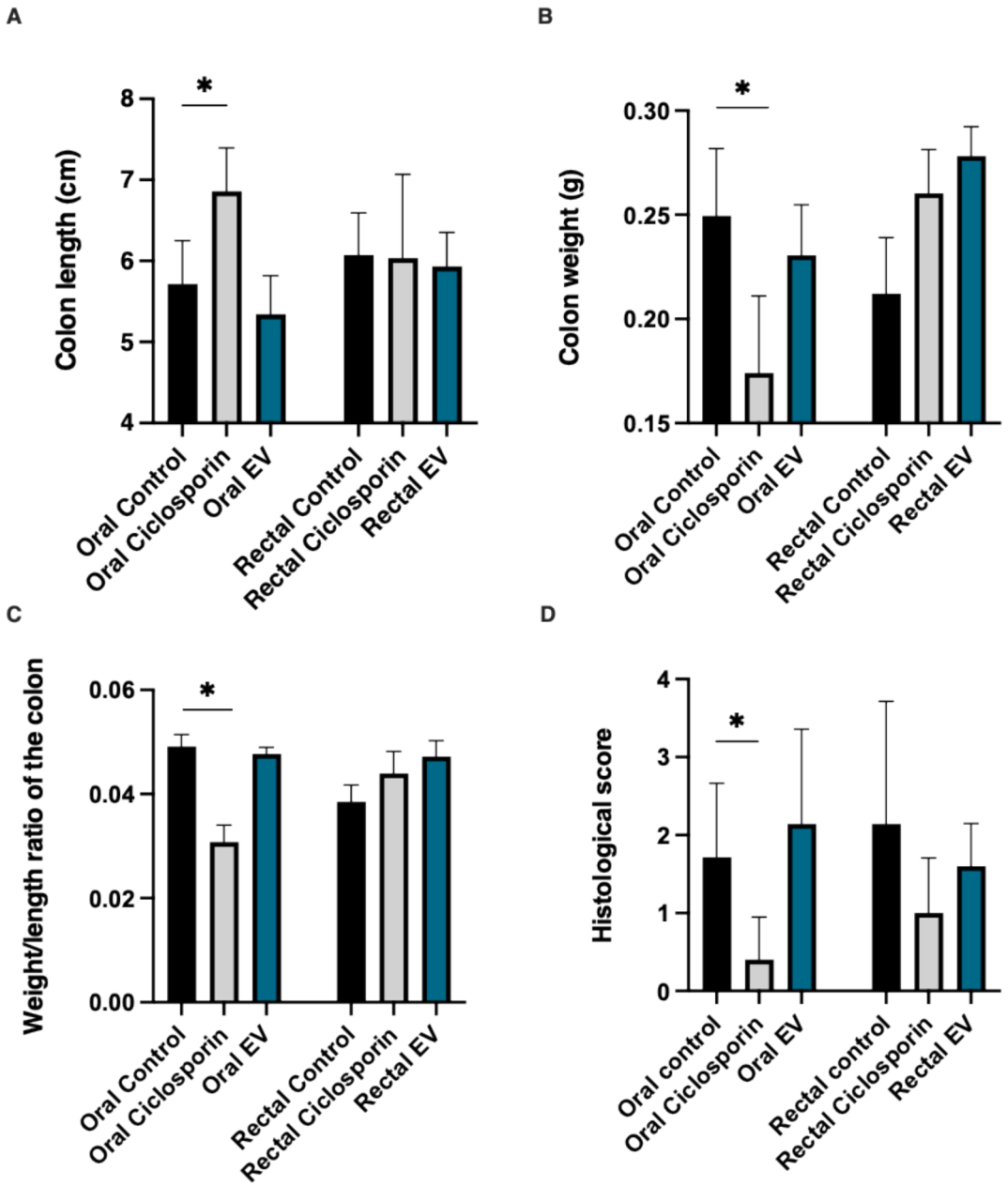

Fig. 11. Bar charts indicating (A) colon length, (B) colon weight, (C) colon weight to length ratio and (D) histological scoring following administration of either EVs, Ciclosporin or PBS by oral or rectal administration (n = 7).

the release study (see Fig. 6**C**) and the *in vivo* study (see Fig. 6**D**).

3.3. Vesicle stability measured via a laurdan fluorescence assay

Milk EVs and liposomes as a positive control were successfully loaded with the fluorescent dye laurdan (2-dimethylamino-6-lauroylnaphthalene) via passive diffusion and exposed to simulated GI fluids. Laurdan is non-fluorescent in water but intercalates into lipid bilayers, exhibiting different emission properties based on the polarity of its environment. Variations in membrane water content cause shifts in the laurdan emission spectrum, quantified by calculating the generalized polarization (GP). Tightly ordered lipids shift the maximum emission spectrum to 435 nm, while a peak at 490 nm indicates a disordered state. The GP index is calculated using the formula: $GP = (I_{435}–I_{490})/(I_{435} + I_{490})$, with values ranging from −0.2 to 0.7. GP values closer to −0.2 indicate an environment with high lipid packing, and a low number of hydrogen bonds (low polarity) in the probe surroundings whereas GP values around 0.7 demonstrate a more polar environment [62]. In the event of lipid bilayer disruption, water penetrates the surface of the bilayer driving laurdan molecules deeper into the bilayer by their hydrophobic lauric acid tail. Since laurdan does not fluoresce in water, the fluorescent signal obtained originates from the deeper bilayer environment where the amount of dipolar relaxation is reduced; thereby displaying an increase in GP values [63,64]. Milk EVs exhibited statistically significant increases in GP values when exposed to PBS at gastric pH ($p < 0.05$), in gastric fluids ($p < 0.01$) and in small intestinal fluid ($p < 0.001$) indicating lipid bilayer damage (Fig. 7). Conversely, GP values decreased in the presence of colonic fluids, which is likely attributed to the presence of surfactants such as Tween 80. These surfactants may localise around the EV membrane, reducing the polarity of the surrounding environment and thus leading to lower GP values. Liposomes were used as a positive control, it is known that liposomes are particularly unstable in gastric and small intestinal fluids, due to the presence of gastric acid, bile salts and pancreatic lipases [65,66]. As expected,

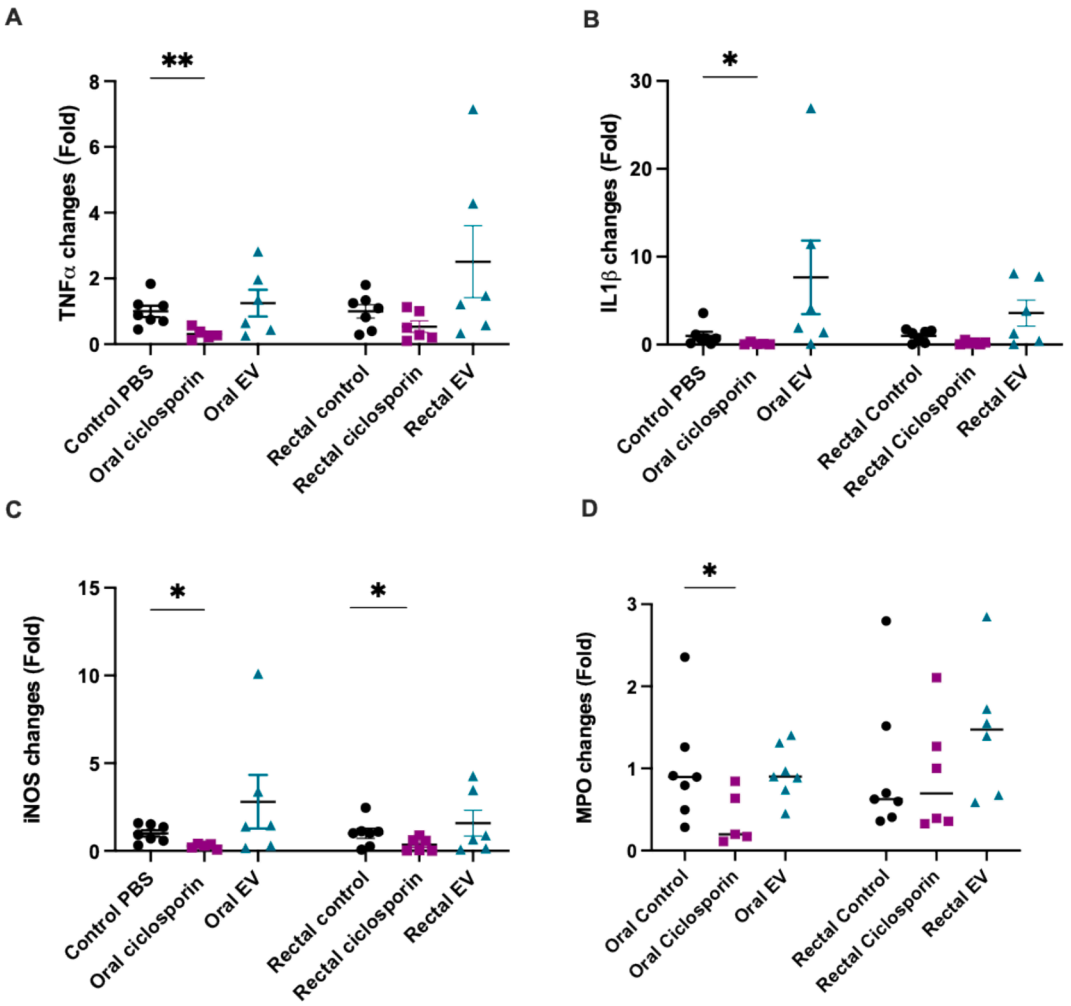

Fig. 12. Scatter plots of qPCR analyses of colonic the inflammatory markers (A) TNFα, (B) IL-1b, (C) iNOS and (D) MPO (n = 7).

liposomes exhibited a significant increase in GP values in the presence of gastric pH and gastric and intestinal fluids but not in the presence of colonic fluids, thereby confirming the reliability of the assay.

In this study, we observed similar trends in lipid bilayer instability for milk EVs and liposomes in the GI environment; given the convenience and cost-effectiveness of isolating bovine milk EVs, they constitute promising carriers for oral drug delivery if used in combination with colon-targeted delivery technologies. These results contrast with studies reporting RNA stability from human or bovine milk EVs under *in vitro* digestion conditions [43,47,51]. Agrawal et al. reported similar drug release profiles in PBS and fed-state GI fluids, but their study used non-acidic gastric pH (pH 5) and lacked enzymes, which doesn't reflect the true gastric conditions [37]. Additionally, Wu et al.'s conclusion that increasing GP values indicate membrane stability conflicts with Parasassi et al.'s work, which links such increases to lipid bilayer damage. Our results and the use of liposomes as a positive control support Parasassi et al.'s interpretation, suggesting that Wu et al.'s conclusions may be incorrect [60,63].

3.4. Vesicle stability measured via drug release

Milk EVs were isolated and loaded with two different types of fluorescent molecules/model drugs: riboflavin, a hydrophilic drug intended to reside in the aqueous core of the EVs, and acridine orange (AO), a lipophilic dye expected to integrate into the lipid bilayer of the EVs. Both molecules exhibit fluorescence when excited at specific wavelengths—450 nm for riboflavin and 490 nm for AO. The emission spectra showed peaks at 525 nm for riboflavin and 530 nm for AO, see **Fig. S3**. The Bligh and Dyer lipid extraction method was utilised to determine the distribution of riboflavin and acridine orange within the EVs and the results are shown in Fig. 8 [57]. It can be seen that most of the riboflavin was located in the aqueous phase, indicating that riboflavin is predominantly situated in the aqueous core of the EVs. In contrast, three quarters of the loaded acridine orange was in the lipid phase and a quarter was in the aqueous core. It is interesting to note that while acridine orange primarily resided within the lipid bilayer of the EVs, a small portion was also present in the aqueous core. These findings confirm the expected localisation of these hydrophilic and lipophilic molecules within the different compartments of the EVs. Our findings are also are in line with reports stating that a small proportion of AO binds to DNA and RNA located within the aqueous EV cores [67].

Upon exposure to simulated gastrointestinal (GI) fluids, milk EVs loaded with riboflavin showed no variations in fluorescence intensity ($p > 0.05$) following exposure to simulated GI fluids, which (Fig. 9**B**) suggests that milk EVs are capable of maintaining their hydrophilic cargo in the simulated GI fluids. In contrast to riboflavin loaded EVs, those loaded with acridine orange (milk EVs_{AO}) exhibited a clear reduction in fluorescence (Fig. 9**A**). One-way ANOVA revealed a significant ($p < 0.05$) difference in fluorescence intensities across the different fluids. Post hoc Tukey tests indicated a significant ($p < 0.05$) decrease in fluorescence at acidic pH and in enzyme-containing simulated fluids, including α-amylase in saliva and pancreatin in intestinal fluids and gastric enzymes in gastric fluid. These findings indicate that milk EVs_{AO} are susceptible to both acidic and enzymatic degradation

and would be unstable in the stomach and in the small intestine, but stable in the colon. This instability for AO at acidic gastric pH and in simulated gastric and small intestinal fluids aligns with the instability observed for the lipophilic probe laurdan.

The observed maintenance of hydrophilic cargo, alongside the loss of lipophilic cargo, suggests that exposure to saliva, low pH, and simulated gastrointestinal fluids alters the fluidity of the EVs' lipid bilayer, leading to leakage of lipophilic compounds. However, these changes in the lipid bilayer are insufficient to cause any loss of hydrophilic cargo within the aqueous EV core. These findings indicate that EVs are ideally suited for the oral delivery of hydrophilic compounds, particularly nucleic acids, which aligns with their preferential capacity to encapsulate hydrophilic biomacromolecule drugs [68]. Alongside laurdan results, these findings collectively underscore the vulnerability of EVs' lipid bilayers to acidic and enzymatic degradation, which leads to the release of encapsulated drugs. Our results are aligned with those of Xu et al., who showed the instability of milk-derived EVs in the stomach. In their study in diabetic mice, a single dose of liraglutide-loaded bovine milk-derived EVs effectively reduced blood glucose levels after sublingual administration, while oral gavage was ineffective [52]. However, Xu et al.'s results also indicate stability of milk EVs in the saliva so that sublingually administered liraglutide-loaded EVs were effective. In this respect, our data with acridine orange loaded milk EVs, which showed significant drug release in saliva fluids contradicts those of Xu et al.'s findings. It is possible that the difference was due to our prolonged incubation for saliva fluids. It is important to note that sublingual absorption is rapid, and the 1-hour incubation time used in this release study may not reflect this rapid absorption. It must also be noted that most studies on the oral stability of EVs have focussed on the stability of hydrophilic cargoes such as milk RNA in EVs isolated from human or bovine milk and have shown partial RNA stability upon EV incubation in simulated GI fluids [43,47,51].

3.5. *In vivo study: EVs by oral gavage and rectal enema in an acute model of colitis*

In this study, an acute model of colitis was induced in mice via oral gavage of 2 % (w/v) dextran sulphate sodium (DSS) over the course of 5 days. Mice were subsequently administered either bovine milk-derived EVs in PBS, ciclosporin in a mixture of olive oil and ethanol (positive control), or PBS (negative control) by oral gavage (100 μL) or rectal enema (50 μL) daily for 8 days. Analysis of body weight variations indicated a significant increase in weight for mice treated with ciclosporin via oral gavage compared to the negative control ($p < 0.05$), whereas no significant effect was observed with rectal enema (Fig. 10). Notably, the administration of milk EVs did not result in any reduction in weight loss or disease activity index (DAI) when delivered either by oral gavage or rectal enema. Interestingly, oral gavage of EVs led to significant weight loss ($p < 0.05$) and an increase in DAI compared to the control PBS ($p < 0.05$).

In colitis mouse models, colon length and weight serve as crucial indicators of disease severity [69,70]. Inflammation in the colon affects muscle tone [71], leading to colon shortening, while swelling due to inflammation results in increased colonic weight [72]. Additionally, the infiltration of immune cells also results in an increase in spleen weight [73,74]. Macroscopic analysis of sacrificed animals revealed distinct outcomes across experimental groups. As expected, treatment with the positive control, ciclosporin, by oral gavage exhibited significant preventive effects on colitis progression, indicated by increase in colon length ($p < 0.05$) and concomitant reductions in colon weight ($p > 0.05$) weight/length ratio ($p < 0.05$) and in histological scores ($p < 0.05$) whilst showing an increase in colon length ($p < 0.05$) indicating the expected efficacy of ciclosporin in maintaining colon integrity Fig. 11 illustrates. In this study, bovine milk derived EVs given by either oral gavage or rectal enema did not show any significant effects in the macroscopic analysis.

Analysis of colonic inflammatory markers via qPCR, as shown in Fig. 12, mirrored the patterns observed in weight variation and macroscopic analyses. Specifically, ciclosporin administered by oral gavage significantly reduced inflammatory markers ($p < 0.05$). In contrast, ciclosporin given rectally, as well as EVs administered either orally or rectally, did not demonstrate significant effects. Overall, these findings indicate that bovine milk-derived EVs do not exert a therapeutic effect in a DSS colitis mouse model.

These results do not indicate any beneficial properties for the treatment of colitis in DSS-induced C57BL/6 female mice when administered orally or rectally. These findings contradict recent studies in genetic and colitis DSS mouse models that reported therapeutic effects following oral gavage administration [39,40]. For instance, Reif et al. (2020) showed that oral gavage of both cow and human milk-derived EVs prevented significant weight loss and colon shortening in a DSS mouse model. Additionally, cow milk EVs significantly decreased inflammatory markers and lymphocyte infiltration scores. Several factors could explain the discrepancies between this study's results and those of previous studies. One study used Balb/c mice, a strain known to resolve colitis spontaneously shortly after the acute phase, which may not accurately reflect the therapeutic potential of EVs [69,75,76]. Furthermore, all previous studies used male mice, which have higher susceptibility to colitis than females [77], making it easier to detect significant improvements. When investigating therapeutic effects, it is crucial to demonstrate efficacy across sexes and in different animal models [77,78]. Moreover, previous studies varied in their outcomes, with some reporting only macroscopic effects and others showing changes in inflammatory markers without consistent data. Additionally, *in vitro* results in this study demonstrated that EVs were unstable in the upper GI tract, raising questions about their efficacy when administered orally. This was further highlighted by a study from Xu et al., which found that liraglutide-loaded milk EVs had no therapeutic effect when given by oral gavage but did when administered sublingually [52]. Moreover, in the study by Zhang et al., milk EVs loaded with siRNA for TNF-α showed a therapeutic effect when given by oral gavage to a colitis rat model, but milk EVs alone did not have an effect [79]. These results suggest that the therapeutic effects observed in some studies may be due to the loaded therapeutic agents rather than the milk EVs themselves. Collectively, this study's results indicate that bovine milk-derived EVs do not have inherent therapeutic effects for the treatment of colitis in the DSS mouse model.

These findings, alongside the apparent stability results from physical characterization assays, suggest that the lipid bilayer of the EVs is degraded by GI fluids, leading to the degradation/release of their cargo while maintaining an apparent physical structure, highlighting that physical characterisation alone does not fully capture the stability of EVs as drug carriers. The results from this release study, combined with the laurdan assay, suggest that milk EVs are unsuitable as carriers for conventional oral drug delivery but show potential for targeted colonic delivery. Since EVs exert their preferential cell uptake abilities via the cargo they contain, particularly their transmembrane proteins, maintaining the integrity of the entire carrier is necessary to exploit the preferential uptake properties of EVs. Therefore, targeted colonic delivery is the only suitable delivery site for EVs.

4. Conclusion

In this study, the stability of bovine milk derived EVs in simulated GI fluids was assessed. Firstly, the physical characteristics of the EVs were evaluated following exposure to the varying pH levels found in the GI tract, which showed no significant changes indicative of instability based on a one-way ANOVA analysis. To specifically assess the effect of enzymes on EVs, they were loaded with laurdan, a polar probe, to examine the stability of the lipid bilayer in GI fluids. The laurdan assay revealed that the lipid bilayer was damaged after exposure to highly acidic environments and to gastric and intestinal fluids. Furthermore,

milk EVs were loaded with two fluorescent small molecules, riboflavin (hydrophilic) and acridine orange (lipophilic) and exposed them to simulated GI fluids. A significant reduction in fluorescence was observed for the lipophilic drug, indicating EV instability, in the presence of saliva, gastric, and intestinal fluids. These findings confirm that EVs are susceptible to acidic and enzymatic degradation, highlighting that physical characterisation alone does not fully capture their stability as drug carriers. *In vivo* studies further demonstrated that bovine milk-derived EVs did not exhibit any beneficial properties for the treatment of colitis in DSS-induced C57BL/6 female mice model when administered orally or rectally. Overall, bovine milk-derived EVs lack intrinsic therapeutic properties for treating colitis and are limited for conventional oral drug delivery but show promise for the oral delivery of hydrophilic compounds if used in combination with colon-targeted delivery technologies.

Data availability:

All data generated or analysed during this study are included in this published article.

CRediT authorship contribution statement

Nidhi Seegobin: Writing – review & editing, Writing – original draft, Visualization, Validation, Project administration, Methodology, Investigation, Funding acquisition, Formal analysis, Data curation, Conceptualization. **Marissa Taub:** Writing – review & editing, Methodology, Investigation, Formal analysis. **Cécile Vignal:** Writing – review & editing, Methodology, Investigation, Formal analysis, Conceptualization. **Christophe Waxin:** Writing – review & editing, Methodology, Investigation. **Victoria Chris:** Writing – review & editing, Methodology, Investigation, Data curation. **Atheer Awad:** Writing – review & editing, Supervision, Methodology. **Sudaxshina Murdan:** Writing – review & editing, Supervision. **Abdul W Basit:** Writing – review & editing, Supervision, Methodology, Conceptualization.

5. Ethics approval and consent to participate

This study was performed in accordance with the approval (Authorisation No. 7267–2016100410284439) from the Ethics Committee in Animal Experimentation Nord-Pas de Calais (CEEA75) which was approved by the French ministry for higher education and research. The CEEA75 carries out its activity according to the principles of European directive 2010/63/EU (transposed into French law 2013/2/1/AGRG1238767A) and the "National Charter on the ethics of animal experimentation" while respecting the recommendations for specific procedures issued by the National Ethics Reflection Committee on animal experimentation. All institutional and national guidelines for the care and use of laboratory animals were followed. As this study did not involve human subjects, consent to participate was not applicable.

Funding Statement

This project received funding from the EPSRC CDT in Transformative Pharmaceutical Technologies grant 'EP/S023054/1′ and the Interreg 2 Seas programme 2014–2020 co-funded by the European Regional Development Fund under subsidy contract "Site Drug 2S07-033".

Declaration of competing interest

The authors declare that they have no known competing financial interests or personal relationships that could have appeared to influence the work reported in this paper.

Acknowledgments

The authors acknowledge the use of BioRender.com in creating Figs. 1-5. The authors thank the staff of the animal facilities of Lille University Hospital (DHURE).

Appendix A. Supplementary data

Supplementary data to this article can be found online at https://doi.org/10.1016/j.ejpb.2025.114744.

Data availability

Data will be made available on request.

References

[1] J.J. Ashton, Z. Green, V. Kolimarala, R.M. Beattie, Inflammatory bowel disease: long-term therapeutic challenges, *Expert Rev. Gastroenterol. Hepatol.* 13 (2019) 1049–1063, https://doi.org/10.1080/17474124.2019.1685872.
[2] Excellence, T.N.I.f.H.a.C. Faecal calprotectin diagnostic tests for inflammatory diseases of the bowel. Available online: (accessed on.
[3] R.B. Sartor, Genetics and Environmental Interactions Shape the Intestinal Microbiome to Promote Inflammatory Bowel Disease Versus Mucosal Homeostasis, *Gastroenterology* 139 (2010) 1816–1819, https://doi.org/10.1053/j.gastro.2010.10.036.
[4] I. Sensoy, A review on the food digestion in the digestive tract and the used in vitro models, *Curr. Res. Food Sci.* 4 (2021) 308–319, https://doi.org/10.1016/j.crfs.2021.04.004.
[5] S. Ahadian, J.A. Finbloom, M. Mofidfar, S.E. Diltemiz, F. Nasrollahi, E. Davoodi, V. Hosseini, I. Mylonaki, S. Sangabathuni, H. Montazerian, et al., Micro and nanoscale technologies in oral drug delivery, *Adv. Drug Deliv. Rev.* 157 (2020) 37–62, https://doi.org/10.1016/j.addr.2020.07.012.
[6] A. Awad, C. Madla, L. McCoubrey, F. Ferraro, F. Gavins, A. Buanz, S. Gaisford, M. Orlu, F. Siepmann, J. Siepmann, et al., Clinical translation of advanced colonic drug delivery technologies, Adv. Drug Deliv. Rev. (2022) 181, https://doi.org/10.1016/j.addr.2021.114076.
[7] L.E. McCoubrey, A. Favaron, A. Awad, M. Orlu, S. Gaisford, A.W. Basit, Colonic drug delivery: Formulating the next generation of colon-targeted therapeutics, J Control Release 353 (2023) 1107–1126, https://doi.org/10.1016/j.jconrel.2022.12.029.
[8] F. Varum, A.C. Freire, H.M. Fadda, R. Bravo, A.W. Basit, A dual pH and microbiota-triggered coating (Phloral™) for fail-safe colonic drug release, Int J Pharm 583 (2020) 119379, https://doi.org/10.1016/j.ijpharm.2020.119379.
[9] X. Li, C. Lu, Y.Y. Yang, C.H. Yu, Y.F. Rao, Site-specific targeted drug delivery systems for the treatment of inflammatory bowel disease, *Biomed. Pharmacother.* 129 (2020) doi:10.1016/j.biopha.2020.110486.
[10] I. Khan, K. Saeed, I. Khan, Nanoparticles: Properties, applications and toxicities, *Arab. J. Chem.* 12 (2019) 908–931, https://doi.org/10.1016/j.arabjc.2017.05.011.
[11] A. Lamprecht, U. Schäfer, C.M. Lehr, Size-dependent bioadhesion of micro- and nanoparticulate carriers to the inflamed colonic mucosa, *Pharm. Res.* 18 (2001) 788–793, https://doi.org/10.1023/a:1011032328064.
[12] H. Ali, B. Weigmann, E.-M. Collnot, S.A. Khan, M. Windbergs, C.-M. Lehr, Budesonide Loaded PLGA Nanoparticles for Targeting the Inflamed Intestinal Mucosa—Pharmaceutical Characterization and Fluorescence Imaging, *Pharm. Res.* 33 (2016) 1085–1092, https://doi.org/10.1007/s11095-015-1852-6.
[13] Z. Wang, J. Shen, The role of goblet cells in Crohn' s disease, *CELL AND BIOSCIENCE* 14 (2024) doi:10.1186/s13578-024-01220-w.
[14] A. Swidsinski, V. Loening-Baucke, F. Theissig, H. Engelhardt, S. Bengmark, S. Koch, H. Lochs, Y. Dörffel, Comparative study of the intestinal mucus barrier in normal and inflamed colon, *Gut* 56 (2007) 343–350, https://doi.org/10.1136/gut.2006.098160.
[15] E. Stange, B. Schroeder, Microbiota and mucosal defense in IBD: an update, *Expert Rev. Gastroenterol. Hepatol.* 13 (2019) 963–976, https://doi.org/10.1080/17474124.2019.1671822.
[16] M. Johansson, Mucus Layers in Inflammatory Bowel Disease, *Inflamm. Bowel Dis.* 20 (2014) 2124–2131, https://doi.org/10.1097/MIB.0000000000000117.
[17] S. Bandi, Y. Kumbhar, V. Venuganti, Effect of particle size and surface charge of nanoparticles in penetration through intestinal mucus barrier, *J. Nanopart. Res.* 22 (2020) doi:10.1007/s11051-020-04785-y.
[18] Z. Akkus, I. Nazir, A. Jalil, M. Tribus, A. Bernkop-Schnürch, Zeta Potential Changing Polyphosphate Nanoparticles: A Promising Approach To Overcome the Mucus and Epithelial Barrier, *Mol. Pharmaceutics* 16 (2019) 2817–2825, https://doi.org/10.1021/acs.molpharmaceut.9b00355.
[19] B. Tirosh, N. Khatib, Y. Barenholz, A. Nissan, A. Rubinstein, Transferrin as a Luminal Target for Negatively Charged Liposomes in the Inflamed Colonic Mucosa, *Mol. Pharmaceutics* 6 (2009) 1083–1091, https://doi.org/10.1021/mp9000926.
[20] M. Carlson, Y. Raab, C. Peterson, R. Hällgren, P. Venge, Increased intraluminal release of eosinophil granule proteins EPO, ECP, EPX, and cytokines in ulcerative colitis and proctitis in segmental perfusion, *Am. J. Gastroenterol.* 94 (1999) 1876–1883.
[21] C. Peterson, E. Eklund, Y. Taha, Y. Raab, M. Carlson, A new method for the quantification of neutrophil and eosinophil cationic proteins in feces: Establishment of normal levels and clinical application in patients with inflammatory bowel disease, *Am. J. Gastroenterol.* 97 (2002) 1755–1762.
[22] K. Witwer, J. Wolfram, Extracellular vesicles versus synthetic nanoparticles for drug delivery, *Nat. Rev. Mater.* 6 (2021) 103–106, https://doi.org/10.1038/s41578-020-00277-6.

[23] I. Mignini, G. Piccirilli, F. Termite, M. Paratore, G. Esposto, L. Laterza, F. Scaldaferri, M.E. Ainora, A. Gasbarrini, M.A. Zocco, Extracellular Vesicles: Novel Potential Therapeutic Agents in Inflammatory Bowel Diseases, *Cells* 13 (2023) doi:10.3390/cells13010090.

[24] Welsh, J.; Goberdhan, D.; O'Driscoll, L.; Buzas, E.; Blenkiron, C.; Bussolati, B.; Cai, H.; Di Vizio, D.; Driedonks, T.; Erdbrügger, U.; et al. Minimal information for studies of extracellular vesicles (MISEV2023): From basic to advanced approaches (vol 13, e12404, 2023). *JOURNAL OF EXTRACELLULAR VESICLES* **2024**, *13*, doi: 10.1002/jev2.12451.

[25] Welsh, J.; Goberdhan, D.; O'Driscoll, L.; Buzas, E.; Blenkiron, C.; Bussolati, B.; Cai, H.; Di Vizio, D.; Driedonks, T.; Erdbrügger, U.; et al. [Minimal information for studies of extracellular vesicles (MISEV2023): From basic to advanced approaches (vol 13, e12404, 2023)]. *JOURNAL OF EXTRACELLULAR VESICLES* **2024**, *13*, doi: 10.1002/jev2.12451.

[26] Y. Zhang, Y. Liu, H. Liu, W. Tang, Exosomes: biogenesis, biologic function and clinical potential, *CELL AND BIOSCIENCE* 9 (2019) doi:10.1186/s13578-019-0282-2.

[27] G. Raposo, W. Stoorvogel, Extracellular vesicles: Exosomes, microvesicles, and friends, *J. Cell Biol.* 200 (2013) 373–383, https://doi.org/10.1083/jcb.201211138.

[28] N.P. Hessvik, A. Llorente, Current knowledge on exosome biogenesis and release, *Cell Mol Life Sci* 75 (2018) 193–208, https://doi.org/10.1007/s00018-017-2595-9.

[29] L.M. Doyle, M.Z. Wang, Overview of Extracellular Vesicles, Their Origin, Composition, Purpose, and Methods for Exosome Isolation and Analysis, *Cells* 8 (2019) 727, https://doi.org/10.3390/cells8070727.

[30] A. Gonda, J. Kabagwira, G. Senthil, N. Wall, Internalization of Exosomes through Receptor-Mediated Endocytosis, *Mol. Cancer Res.* 17 (2019) 337–347, https://doi.org/10.1158/1541-7786.MCR-18-0891.

[31] D.E. Murphy, O.G. de Jong, M.J.W. Evers, M. Nurazizah, R.M. Schiffelers, P. Vader, Natural or Synthetic RNA Delivery: A Stoichiometric Comparison of Extracellular Vesicles and Synthetic Nanoparticles, *Nano Lett* 21 (2021) 1888–1895, https://doi.org/10.1021/acs.nanolett.1c00094.

[32] J.L. Betker, B.M. Angle, M.W. Graner, T.J. Anchordoquy, The Potential of Exosomes From Cow Milk for Oral Delivery, *J. Pharm. Sci.* 108 (2019) 1496–1505, https://doi.org/10.1016/j.xphs.2018.11.022.

[33] G. Carobolante, J. Mantaj, E. Ferrari, D. Vllasaliu, Cow Milk and Intestinal Epithelial Cell-derived Extracellular Vesicles as Systems for Enhancing Oral Drug Delivery, *Pharmaceutics* 12 (2020) doi:10.3390/pharmaceutics12030226.

[34] T. Wolf, S.R. Baier, J. Zempleni, The Intestinal Transport of Bovine Milk Exosomes Is Mediated by Endocytosis in Human Colon Carcinoma Caco-2 Cells and Rat Small Intestinal IEC-6 Cells, *J. Nutr.* 145 (2015) 2201–2206, https://doi.org/10.3945/jn.115.218586.

[35] R.J. Kusuma, S. Manca, T. Friemel, S. Sukreet, C. Nguyen, J. Zempleni, Human vascular endothelial cells transport foreign exosomes from cow's milk by endocytosis, *Am J Physiol Cell Physiol* 310 (2016) C800–C807, https://doi.org/10.1152/ajpcell.00169.2015.

[36] M.R. Warren, C. Zhang, A. Vedadghavami, K. Bokvist, P.K. Dhal, A.G. Bajpayee, Milk exosomes with enhanced mucus penetrability for oral delivery of siRNA, *Biomater Sci* 9 (2021) 4260–4277, https://doi.org/10.1039/d0bm01497d.

[37] A.K. Agrawal, F. Aqil, J. Jeyabalan, W.A. Spencer, J. Beck, B.W. Gachuki, S. S. Alhakeem, K. Oben, R. Munagala, S. Bondada, et al., Milk-derived exosomes for oral delivery of paclitaxel, *Nanomedicine* 13 (2017) 1627–1636, https://doi.org/10.1016/j.nano.2017.03.001.

[38] L. Tong, H. Hao, Z. Zhang, Y. Lv, X. Liang, Q. Liu, T. Liu, P. Gong, L. Zhang, F. Cao, et al., Milk-derived extracellular vesicles alleviate ulcerative colitis by regulating the gut immunity and reshaping the gut microbiota, *Theranostics* 11 (2021) 8570–8586, https://doi.org/10.7150/thno.62046.

[39] W. Stremmel, R. Weiskirchen, B.C. Melnik, Milk Exosomes Prevent Intestinal Inflammation in a Genetic Mouse Model of Ulcerative Colitis: A Pilot Experiment, *Inflamm Intest Dis* 5 (2020) 117–123, https://doi.org/10.1159/000507626.

[40] S. Reif, Y. Elbaum-Shiff, N. Koroukhov, I. Shilo, M. Musseri, R. Golan-Gerstl, Cow and Human Milk-Derived Exosomes Ameliorate Colitis in DSS Murine Model, *Nutrients* 12 (2020) 2589, https://doi.org/10.3390/nu12092589.

[41] A. Jash, A. Ubeyitogullari, S.S.H. Rizvi, Liposomes for oral delivery of protein and peptide-based therapeutics: challenges, formulation strategies, and advances, *J. Mat. Chem. B* 9 (2021) 4773–4792, https://doi.org/10.1039/D1TB00126D.

[42] W. Wu, Y. Lu, J. Qi, Oral Delivery of Liposomes. (2015), https://doi.org/10.4155/tde.15.69.

[43] H. Izumi, N. Kosaka, T. Shimizu, K. Sekine, T. Ochiya, M. Takase, Bovine milk contains microRNA and messenger RNA that are stable under degradative conditions, *J. Dairy Sci.* 95 (2012) 4831–4841, https://doi.org/10.3168/jds.2012-5489.

[44] P. Rani, M. Vashisht, N. Golla, S. Shandilya, S.K. Onteru, D. Singh, Milk miRNAs encapsulated in exosomes are stable to human digestion and permeable to intestinal barrier in vitro, *J. Funct. Foods* 34 (2017) 431–439, https://doi.org/10.1016/j.jff.2017.05.009.

[45] S. Kahn, Y. Liao, X. Du, W. Xu, J. Li, B. Lönnerdal, Exosomal MicroRNAs in Milk from Mothers Delivering Preterm Infants Survive in Vitro Digestion and Are Taken Up by Human Intestinal Cells, *Mol. Nutr. Food Res.* 62 (2018) 1701050, https://doi.org/10.1002/mnfr.201701050.

[46] A. Benmoussa, C.H.C. Lee, B. Laffont, P. Savard, J. Laugier, E. Boilard, C. Gilbert, I. Fliss, P. Provost, Commercial Dairy Cow Milk microRNAs Resist Digestion under Simulated Gastrointestinal Tract Conditions, *J. Nutr.* 146 (2016) 2206–2215, https://doi.org/10.3945/jn.116.237651.

[47] Y. Liao, X. Du, J. Li, B. Lönnerdal, Human milk exosomes and their microRNAs survive digestion in vitro and are taken up by human intestinal cells, *Mol. Nutr. Food Res.* 61 (2017) 1700082, https://doi.org/10.1002/mnfr.201700082.

[48] R. Munagala, F. Aqil, J. Jeyabalan, R.C. Gupta, Bovine milk-derived exosomes for drug delivery, *Cancer Lett.* 371 (2016) 48–61, https://doi.org/10.1016/j.canlet.2015.10.020.

[49] C.H. Yang, M.Z. Zhang, J. Sung, L.X. Wang, Y.J. Jung, D. Merlin, Autologous Exosome Transfer: A New Personalised Treatment Concept to Prevent Colitis in a Murine Model, *Journal of Crohns & Colitis* 14 (2020) 841–855, https://doi.org/10.1093/ecco-jcc/jjz184.

[50] D. Donoso-Meneses, A. Figueroa-Valdes, M. Khoury, F. Alcayaga-Miranda, Oral Administration as a Potential Alternative for the Delivery of Small Extracellular Vesicles, *PHARMACEUTICS* 15 (2023) doi:10.3390/pharmaceutics15030716.

[51] López de las Hazas, M.-C.; del Pozo-Acebo, L.; Hansen, M.S.; Gil-Zamorano, J.; Mantilla-Escalante, D.C.; Gómez-Coronado, D.; Marín, F.; Garcia-Ruiz, A.; Rasmussen, J.T.; Dávalos, A. Dietary bovine milk miRNAs transported in extracellular vesicles are partially stable during GI digestion, are bioavailable and reach target tissues but need a minimum dose to impact on gene expression. *Eur J Nutr* **2022**, *61*, 1043-1056, doi:10.1007/s00394-021-02720-y.

[52] M. Xu, G. Chen, Y. Dong, J. Yang, Y. Liu, H. Song, H. Song, Y. Wang, Liraglutide-Loaded Milk Exosomes Lower Blood Glucose When Given by Sublingual Route, *ChemMedChem* 17 (2022) e202100758, https://doi.org/10.1002/cmdc.202100758.

[53] K. Vaswani, Y.Q. Koh, F.B. Almughlliq, H.N. Peiris, M.D. Mitchell, A method for the isolation and enrichment of purified bovine milk exosomes, *Reprod. Biol.* 17 (2017) 341–348, https://doi.org/10.1016/j.repbio.2017.09.007.

[54] J. Ali, J. Bong Lee, S. Gittings, A. Iachelini, J. Bennett, A. Cram, M. Garnett, C. J. Roberts, P. Gershkovich, Development and optimisation of simulated salivary fluid for biorelevant oral cavity dissolution, *Eur J Pharm Biopharm* 160 (2021) 125–133, https://doi.org/10.1016/j.ejpb.2021.01.017.

[55] J. Wang, V. Yadav, A.L. Smart, S. Tajiri, A.W. Basit, Toward oral delivery of biopharmaceuticals: an assessment of the gastrointestinal stability of 17 peptide drugs, *Mol Pharm* 12 (2015) 966–973, https://doi.org/10.1021/mp500809f.

[56] S. Klein, The Use of Biorelevant Dissolution Media to Forecast the In Vivo Performance of a Drug, *AAPS J* 12 (2010) 397–406, https://doi.org/10.1208/s12248-010-9203-3.

[57] Bligh, E.G.; Dyer, W.J. A rapid method of total lipid extraction and purification. **1959**.

[58] N. Hanning, J.G. De Man, B.Y. De Winter, Measuring Myeloperoxidase Activity as a Marker of Inflammation in Gut Tissue Samples of Mice and Rat, BioProtoc 13 (2023) e4758.

[59] I. Sensoy, A review on the food digestion in the digestive tract and the used in vitro models, *Curr. Res. Food Sci.* 4 (2021) 308–319, https://doi.org/10.1016/j.crfs.2021.04.004.

[60] L. Wu, L. Wang, X. Liu, Y. Bai, R. Wu, X. Li, Y. Mao, L. Zhang, Y. Zheng, T. Gong, et al., Milk-derived exosomes exhibit versatile effects for improved oral drug delivery, *Acta Pharm. Sin. B* 12 (2022) 2029–2042, https://doi.org/10.1016/j.apsb.2021.12.015.

[61] T. Skotland, K. Ekroos, A. Llorente, K. Sandvig, Quantitative Lipid Analysis of Extracellular Vesicle Preparations: A Perspective, *J Extracell Vesicles* 14 (2025) e70049, https://doi.org/10.1002/jev2.70049.

[62] S. Palleschi, L. Silvestroni, Laurdan fluorescence spectroscopy reveals a single liquid-crystalline lipid phase and lack of thermotropic phase transitions in the plasma membrane of living human sperm, *Biochim Biophys Acta* 1279 (1996) 197–202, https://doi.org/10.1016/0005-2736(95)00250-2.

[63] T. Parasassi, E.K. Krasnowska, L. Bagatolli, E. Gratton, Laurdan and Prodan as Polarity-Sensitive Fluorescent Membrane Probes, *J. Fluoresc.* 8 (1998) 365–373, https://doi.org/10.1023/A:1020528716621.

[64] T. Parasassi, A.M. Giusti, E. Gratton, E. Monaco, M. Raimondi, G. Ravagnan, O. Sapora, Evidence for an Increase in Water Concentration in Bilayers after Oxidative Damage of Phospholipids Induced by Ionizing Radiation, *Int. J. Radiat Biol.* 65 (1994) 329–334, https://doi.org/10.1080/09553009414550391.

[65] H. He, Y. Lu, J. Qi, Q. Zhu, Z. Chen, W. Wu, Adapting liposomes for oral drug delivery, *Acta Pharm Sin B* 9 (2019) 36–48, https://doi.org/10.1016/j.apsb.2018.06.005.

[66] M.-K. Lee, Liposomes for Enhanced Bioavailability of Water-Insoluble Drugs: In Vivo Evidence and Recent Approaches, *Pharmaceutics* 12, 264 (2020) doi:10.3390/pharmaceutics12030264.

[67] E. Iessi, M. Logozzi, L. Lugini, T. Azzarito, C. Federici, E.P. Spugnini, D. Mizzoni, R. Di Raimo, D.F. Angelini, L. Battistini, et al., Acridine Orange/exosomes increase the delivery and the effectiveness of Acridine Orange in human melanoma cells: A new prototype for theranostics of tumors, *J Enzyme Inhib Med Chem* 32 (2017) 648–657, https://doi.org/10.1080/14756366.2017.1292263.

[68] Y. Li, L. Xing, L. Wang, X. Liu, L. Wu, M. Ni, Z. Zhou, L. Li, Y. Huang, Milk-derived exosomes as a promising vehicle for oral delivery of hydrophilic biomacromolecule drugs, *Asian J Pharm Sci* 18 (2023) 100797, https://doi.org/10.1016/j.ajps.2023.100797.

[69] C. Yang, D. Merlin, Unveiling Colitis: A Journey through the Dextran Sodium Sulfate-induced Model, *Inflamm Bowel Dis* (2024), https://doi.org/10.1093/ibd/izad312.

[70] B. Chassaing, G. Srinivasan, M.A. Delgado, A.N. Young, A.T. Gewirtz, M. Vijay-Kumar, Fecal lipocalin 2, a sensitive and broadly dynamic non-invasive biomarker for intestinal inflammation, *PLoS One* 7 (2012) e44328, https://doi.org/10.1371/journal.pone.0044328.

[71] L. Börjesson, F. Aldenborg, D.S. Delbro, Functional effects of dextran sulphate sodium (DSS) treatment on the longitudinal muscle of rat distal colon, *J Auton Pharmacol* 21 (2001) 121–129, https://doi.org/10.1046/j.1365-2680.2001.00218.x.

[72] L. Schwartz, M. Abolhassani, M. Pooya, J.M. Steyaert, X. Wertz, M. Israël, A. Guais, P. Chaumet-Riffaud, Hyperosmotic stress contributes to mouse colonic inflammation through the methylation of protein phosphatase 2A, *Am J Physiol Gastrointest Liver Physiol* 295 (2008) G934–G941, https://doi.org/10.1152/ajpgi.90296.2008.

[73] B. Chassaing, J.D. Aitken, M. Malleshappa, M. Vijay-Kumar, Dextran sulfate sodium (DSS)-induced colitis in mice, *Curr Protoc Immunol* 104 (2014) 15.25.11-15.25.14, https://doi.org/10.1002/0471142735.im1525s104.

[74] Y. Shim, A. Weliwitigoda, T. Campbell, M. Dosanjh, P. Johnson, Splenic erythroid progenitors decrease TNF-α production by macrophages and reduce systemic inflammation in a mouse model of T cell-induced colitis, *Eur. J. Immunol.* 51 (2021) 567–579, https://doi.org/10.1002/eji.202048687.

[75] F. Yang, D. Wang, Y. Li, L. Sang, J. Zhu, J. Wang, B. Wei, C. Lu, X. Sun, Th1/Th2 Balance and Th17/Treg-Mediated Immunity in relation to Murine Resistance to Dextran Sulfate-Induced Colitis, *J Immunol Res* 2017 (2017) 7047201, https://doi.org/10.1155/2017/7047201.

[76] T. Tsuchiya, S. Fukuda, H. Hamada, A. Nakamura, Y. Kohama, H. Ishikawa, K. Tsujikawa, H. Yamamoto, Role of γδT cells in the inflammatory response of experimental colitis mice, *J. Immunol.* 171 (2003) 5507–5513.

[77] J. Bábíková, L. Tóthová, E. Lengyelová, A. Bartonová, J. Hodosy, R. Gardlík, P. Celec, Sex Differences in Experimentally Induced Colitis in Mice: a Role for Estrogens, *Inflammation* 38 (2015) 1996–2006, https://doi.org/10.1007/s10753-015-0180-7.

[78] D. Low, D. Nguyen, E. Mizoguchi, Animal models of ulcerative colitis and their application in drug research, *Drug Des. Dev. Ther.* 7 (2013) 1341–1356, https://doi.org/10.2147/DDDT.S40107.

[79] Y. Zhang, M. Belaid, X. Luo, A. Daci, R. Limani, J. Mantaj, M. Zilbauer, K. Nayak, D. Vllasaliu, Probing milk extracellular vesicles for intestinal delivery of RNA therapies, *J Nanobiotechnology* 21 (2023) 406, https://doi.org/10.1186/s12951-023-02173-x.